

Coumarin-bisureas as potent fluorescent transmembrane anion transporters

Mohamed Fares,^{a,b,c} Xin Wu,^a Daniel A. McNaughton,^a Alexander M. Gilchrist,^a William Lewis,^a Paul A. Keller,^b Alain Arias-Betancur,^{d,e} Ricardo Pérez-Tomás^d, Philip A. Gale,^{*a,f}

A series of fluorescent coumarin bis-ureas have been synthesised and their anion transport properties studied. The compounds function as highly potent HCl co-transport agents in lipid bilayer membranes.

The transport of ions across phospholipid bilayer membranes in biological systems is a crucial process in many biological processes including, cell migration and proliferation, and maintaining cellular pH, membrane potential and cellular secretions.^[1] Channelopathies are a group of diseases characterised by ion channel impairment, which include cystic fibrosis, epilepsy and cancer.^[2] For example, cystic fibrosis transmembrane conductance regulator (CFTR) is a channel present in epithelial cells that is responsible for facilitating the transport of chloride and bicarbonate through the cell membrane. Dysfunctional CFTR channels with reduced anion transport caused chronic lung infections in cystic fibrosis patients, while impairment of sodium, potassium and T-type calcium channels is linked with epilepsy.^[3] Channel replacement therapy has been proposed as a new approach to treating channelopathies in which the function of a faulty channel is replaced by an ionophore that can facilitate the flux of ions through a membrane by forming a lipophilic complex.^[4]

A number of anionophores and anion exchangers show anti-cancer activity, including the natural product prodigiosin, squaramide derivatives and *o*-phenylenediamine-based bis-ureas.^[5] Studies have shown that chloride transporters can trigger apoptosis in cells whilst compounds that can co-transport H⁺/Cl⁻ can also interfere with autophagy presumably by deacidifying acidic organelles.^[5a, 6] However, our understanding of the action of anionophores within cells is still limited with some studies showing particular classes of

compounds show toxicity whilst other studies show little toxicity but potent anion transport properties.^[2c, 5a, 6-7]

A previous study based on a series of fluorescent (thio)urea-based anionophores was conducted to further understand where anionophores localise in cells using fluorescence imaging techniques.^[8] However, these mono-(thio)urea transporters showed modest anion binding and transport activities.^[8-9] We have conducted another study using squaramide-based fluorescent anionophores to investigate the anion transport activity in the A549 cancer cell line.^[10] However, these compounds ($\log P = 4.9-5.8$) elicited attenuated transport activity compared to the parent squaramide derivatives presumably due to replacing one of the active aniline moiety (containing acidic NH that interacts with the anion) with a bulky naphthalimide fluorophore.

To further improve the anion transport properties and to develop potent fluorescent anion transporters that can be used at lower doses, we designed and synthesized new fluorescent 4-methylcoumarin-bisureas conjugates **1-4** (Fig. 1). We have previously shown that *ortho*-phenylene diamine based bisureas are highly potent anion transporters.^[5d, 5e, 11]

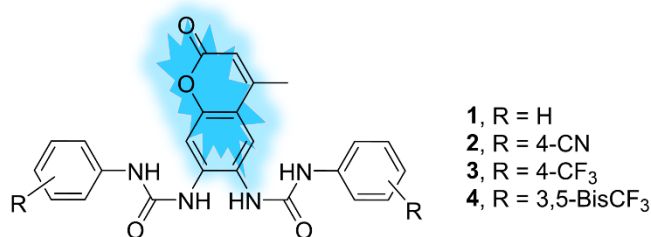


Fig. 1 Structure of designed fluorescent transporters **1-4**

The 4-methylcoumarin scaffold is a small molecular weight fluorophore (more anion binding moieties can be added) with extended spectral range, high emission quantum yields and

^a School of Chemistry, The University of Sydney, NSW 2006, Australia. E-mail: philip.gale@sydney.edu.au

^b School of Chemistry & Molecular Bioscience, Molecular Horizons, University of Wollongong, and Illawarra Health & Medical Research Institute Wollongong, NSW 2522, Australia.

^c Department of Pharmaceutical Chemistry, Faculty of Pharmacy, Egyptian Russian University, Cairo 11829, Egypt

^d Department of Pathology and Experimental Therapeutics, Faculty of Medicine and Health Sciences, Universitat de Barcelona, 08905 Barcelona, Spain

^e Department of Integral Adult Dentistry, Research Centre for Dental Sciences (CICO), Universidad de La Frontera, Temuco 4811230, Chile

^f The University of Sydney Nano Institute (SydneyNano), The University of Sydney, NSW 2006, Australia.

confers the advantage of better solubility than 1,8-naphthalimide fluorophore. The anion binding and transport activities were evaluated for transporters **1-4**. This was followed by investigation of their *in vitro* cytotoxic effects.

The synthetic strategy started with protection of amino group in *m*-aminophenol using ethyl chloroformate to afford ethyl(3-hydroxyphenyl)carbamate **5** (96% yield), which was used in the next step without any further purification.^[12] 7-Carboethoxyamino-4-methylcoumarin **6** was prepared in 75% yield by application of von Pechmann condensation of compound **5** and ethyl acetoacetate in 70% sulfuric acid.^[12] Nitration of **6** using aluminium nitrate nonahydrate in acetic anhydride gave two isomers of nitro 7-carboethoxyamino-4-methylcoumarin, which were separated by flash column chromatography to afford the desired 6-nitro-7-carboethoxyamino-4-methylcoumarin **7** in 36% yield. Compound **7** was hydrolysed under standard acidic conditions to achieve 6-nitro-7-amino-4-methylcoumarin **8** (80% yield), which was reduced using tin/HCl as reported to give the key intermediate 6,7-diamino-4-methylcoumarin **9**, in 36% yield.^[13]

Transporters **1**, **2** and **4** were prepared by nucleophilic addition of the 6,7-diamino-4-methylcoumarin **9** with the corresponding aryl isocyanate in DCM overnight at 45 °C under an inert atmosphere. Interestingly, attempts to prepare transporter **3** using the same procedure failed. Optimization of the reaction involved using different solvents (no solvent, toluene, DMSO and CHCl₃), changing the reaction temperature and using a base. The optimal conditions were found by using no solvent and adding excess of the 4-trifluoromethylphenyl isocyanate under inert condition. By applying these conditions, transporter **3** was obtained, however in a low yield (22%). The structure of compound **1** was confirmed by single crystal X-ray diffraction (Figure 2, see SI). Single crystals were obtained by slow evaporation of a DMF/ethanol solution of **1** at room temperature. The crystal structure (Fig. 2) showed that coumarin rings are stacked on the top of each other in an antiparallel manner and stabilized by the intermolecular hydrogen bonds (see ESI for more details).

The anion binding abilities of potential transporters **1-4** in solution were investigated using ¹H-NMR titration studies in DMSO-*d*₆/0.5% H₂O with tetrabutylammonium chloride. The change in chemical shift of the four urea NHs against the equivalents of anion added was fitted globally to 1:1 (for transporter **1**) and 1:2 (host: guest, for transporters **2-4**) binding modes using BindFit.^[14] The results demonstrate moderately 1:1 chloride affinity in the range of 50 – 250 M⁻¹ in this highly competitive media similar to the previously reported *o*-phenylenebisureas.

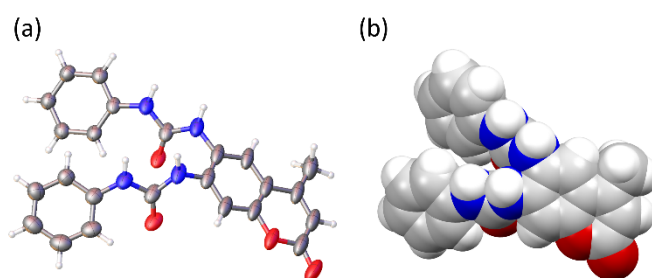


Fig. 2 X-ray crystal structure of **1** (a) ORTEP diagram showing 50% probability anisotropic displacement ellipsoids at 100 K. b-space-filling models.

Receptors **1-4** were investigated for their chloride transport properties across lipid bilayer *via* liposome-based techniques using a chloride ion selective electrode (ISE) (Fig. 3a, Table 1). Briefly, unilamellar POPC vesicles with diameter 200 nm were prepared as reported and loaded with 489 mM KCl, buffered to pH = 7.2 and suspended in 489 Mm KNO₃ solution which is buffered to pH = 7.2. The chloride efflux, as indication of Cl⁻/NO₃⁻ exchange process, was measured using ISE upon addition of DMSO solution of transporters **1-4** to the prepared liposomes.^[9]

Hill plots were performed by monitoring chloride efflux at different concentrations of tested compounds (expressed as mol% with respect to lipid concentration) to calculate EC₅₀ (defined as the concentration required to achieve 50% the chloride efflux at 270 s) and Hill coefficient. The EC₅₀ is used as a measure of anion transporter potency, while Hill coefficient has been linked to the stoichiometry of the formed complex during the transport across the lipid bilayer.^[15] As illustrated in Table 1 and Fig. 3, the unsubstituted coumarin-bisureas hybrid **1** emerged as the least active transporter with EC₅₀ = 4.3 × 10⁻¹ mol%, followed by transporter **4** (EC₅₀ = 1.5 × 10⁻² mol%) (Fig. 3d, Table 1). Transporters **2** and **3**, with *p*-CN and *p*-CF₃ substituents respectively, emerged as the most active transporters with low EC₅₀ values of 7.0 × 10⁻³ and 7.4 × 10⁻³ mol% respectively. Transporters **2-4** (EC₅₀ = 1.5 × 10⁻² - 7.0 × 10⁻³ mol%) (Fig. 3d, Table 1) showed superior transport activity across the lipid bilayer than the previously reported fluorescent naphthalimide-(thio)ureas with at least 10 times lower EC₅₀ values.^[8, 10]

By utilizing the cationophore coupled-KCl assay,^[9] valinomycin (VIn) or monensin (Mon) were used to investigate the mechanism of anion transport of the fluorescent transporters **1-4** (Fig. 3b-c, see SI). This assay was used to determine whether the anionophore transports only chloride in a uniport process resulting in a net flow of charge across the membrane (an electrogenic transporter) if the anionophore couples to valinomycin, or if the anionophore couples to monensin it shows it is functioning as an H⁺/Cl⁻ cotransporter resulting in an electroneutral transport process (no net flow of charge).

Table 1. Transport and anion binding properties of compounds 1–4.

	1	2	3	4	
Binding properties	$^{\circ}\log P$ [a]	3.67	-	-	-
	1:1 (K_s), DMSO- d_6 /0.5% H_2O	81	-	-	-
	covfit [b]	4.6×10^{-4}	-	-	-
	1:2 (K_s), DMSO- d_6 /0.5% H_2O	-	K_{11} : 186; K_{12} : 2	K_{11} : 239; K_{12} : 9	K_{11} : 178; K_{12} : 5
	β_{21} [c]	-	372	2.2×10^3	890
Covfit [b]	-	1.8×10^{-4}	2.0×10^{-4}	3.2×10^{-4}	
Transport properties	Cl/ NO_3 (EC_{50} , mol%) [d]	4.3×10^{-1}	7.0×10^{-3}	7.4×10^{-3}	1.5×10^{-2}
	n [e]	1.2	1.2	1.2	0.93
	KCl (EC_{50} , mol%) [f]	3.8×10^{-2}	5.1×10^{-4}	6.3×10^{-4}	9.7×10^{-4}
	n [e]	0.99	1.2	1.2	1.1

[a] $^{\circ}\log P$ values calculated using VCCLab. [b] The covariance of the fit (covfit) is calculated by dividing the covariance of the residual (experimental data – calculated data) with the covariance of the experimental data. [c] The association constant (β_{21}) for the 2:1 and 1:2 host:guest complex calculated by multiplying K_{11} and K_{12} and K_{11} and K_{21} , respectively. [d] EC_{50} from the Cl/ NO_3 exchange assay. [e] Hill coefficient as an indicator of the stoichiometry the complex mediating transport. [f] EC_{50} from the KCl assay measuring H^+ /Cl $^-$ symport.

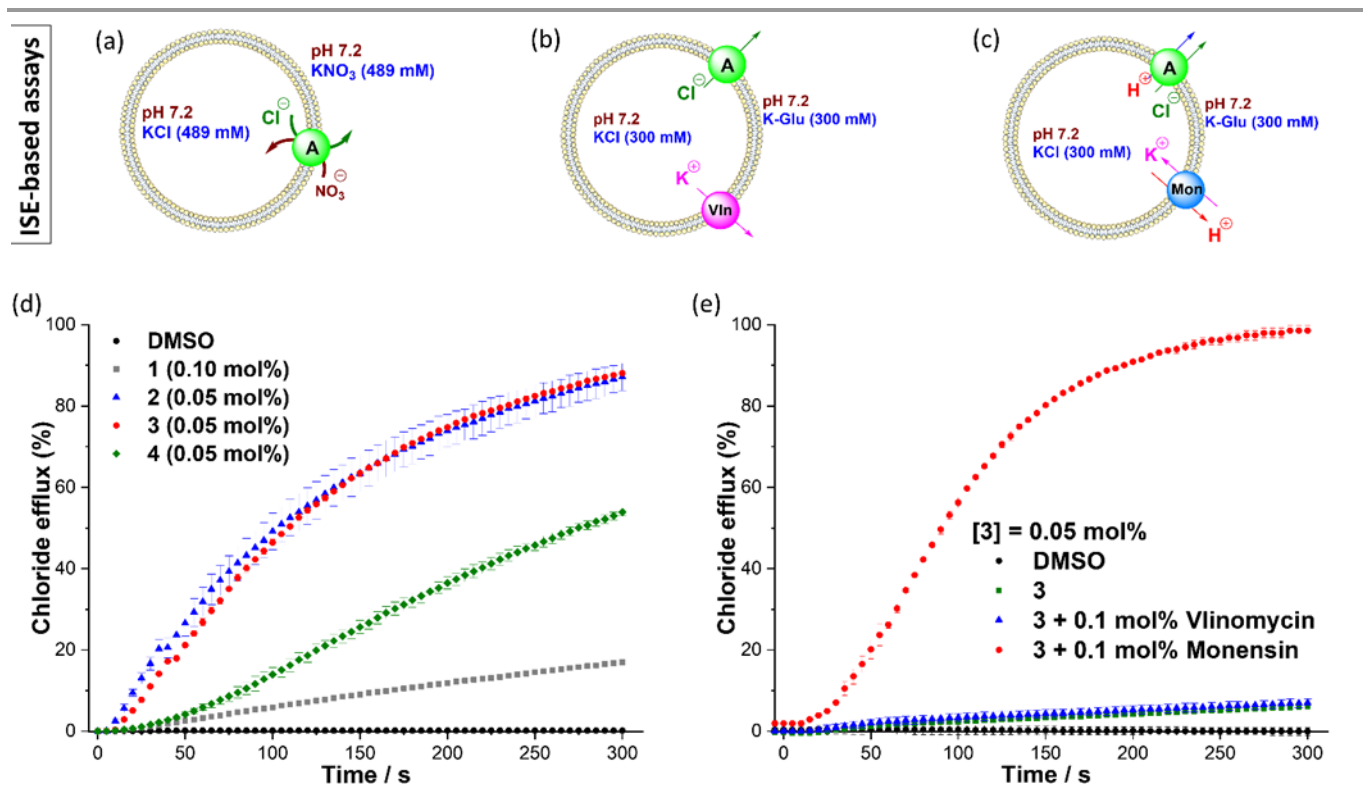


Fig. 3 (a-c) Schematic representation of ISE-based assays used to investigate the mechanism of anion transport of receptors 1-4 (a) Cl/ NO_3 antiport, (b) and (c) cationophore coupled-KCl, valinomycin and monensin to measure the Cl $^-$ uniport and M $^+$ /Cl $^-$ transport, respectively. (d) Chloride efflux achieved by transporters 1-4 (0.10 mol% for transporter 1 and 0.05 mol% for transporters 2-4) from unilamellar POPC vesicles containing 489 mM KCl buffered to pH 7.2 with 5 mM potassium phosphate salts, suspended in 489 mM KNO₃ buffered to pH 7.2 with 5 mM phosphate salts. At the endpoint of each experiment (300 s), the detergent (Triton X-100) was added to lyse the vesicles and calibrate the electrode to 100% chloride efflux. Each point represents the average of at least two trials. DMSO was used as a control experiment (e) Chloride efflux achieved by transporter 3 at 0.05 mol% (rti) in the absence or presence of cationophores (monensin or valinomycin) monitored over a period of 5 min (see SI for more description).

If the anionophore couples to both cationophores it is unselective and can facilitate either chloride uniport or HCl symport (Fig. 3). Compounds 1-4 were found to be highly efficient electroneutral H^+ /Cl $^-$ co-transporters (Fig. 3e, see SI), while transporter 1 is less selective and can also function as a chloride uniporter. The selectivity for HCl co-transport may be the result of the high affinity of the bis-urea motif for phosphate resulting in strong phospholipid headgroup interactions (which

is presumably lower for transporter 1 which lacks electron withdrawing substituents).^[16]

The unsubstituted bisurea-based fluorescent receptor 1 was found to have the lowest activity in HPTS-KCl (HCl symport, Fig. S23) with $EC_{50} = 3.8 \times 10^{-2}$ mol%. Appending electron withdrawing groups increased the ability to dissipate the pH gradient, with $EC_{50} = 5.1 - 9.7 \times 10^{-4}$ mol% (Table 1). The addition of the K $^+$ transporter valinomycin or proton transporter CCCP

did not significantly affect the transport rates of **1-4** in the HPTS assay, consistent with the inability of these compounds to facilitate uniport processes.

The transport of fatty acid carboxylates across lipid bilayer membranes by anionophores can result in pH dissipation across the bilayer as the transported carboxylate protonates and then diffuses back across the bilayer and deprotonates. We used oleic acid (1 mol%) (as a source of fatty acid) and BSA (bovine serum albumin) to sequester fatty acids from liposomes in HPTS-KCl (HCl symport) to investigate whether the fatty acids could play a role in the pH dissipation facilitated by receptors **1-4**. The addition of fatty acid lowered the transport activity of tested compounds **1-4**, which is presumably due to their ability to competitively bind to the carboxylate headgroups as reported^[5d] and thus lowering the chloride transport activity. BSA-treated liposomes were used to remove all fatty acids from the HPTS-KCl liposomes. Transport activity of the fluorescent receptors **1-3** was not affected by the fatty acid removal, suggesting that these transporters independently could transport HCl or protons. However, transporter **4** showed an increase in the pH dissipation which might indicate that the activity of this particular receptor is greatly compromised by the presence of fatty acids.

Cytotoxicity studies on human lung carcinoma cells (A549), human colon adenocarcinoma cells (SW620) and human breast adenocarcinoma cells (MCF-7) were investigated using the MTT assay. Surprisingly, only the most lipophilic compound **4** showed a significant cytotoxicity against all tested cell lines. Compound **4** showed the most cytotoxic effects against SW620 cells ($IC_{50} = 0.51 \pm 0.07$) followed by A549 cells ($IC_{50} = 1.86 \pm 0.39$) and MCF-7 cells ($IC_{50} = 17.92 \pm 4.25$). Further biological studies are currently underway to study the fluorescent behaviour of these anion transporters in cells using confocal fluorescent microscopy techniques.

In conclusion, we designed and synthesized a series of novel bisureas-anion transporters bearing the fluorescent 4-methyl coumarin. The fluorescent anion receptors were tested for their anion binding properties in solution and elicited a relatively strong chloride binding affinity in DMSO-*d*₆/0.5%*H*₂O. These receptors showed a superior Cl⁻/NO₃⁻ exchange ability in ISE-based affinity and H⁺/Cl⁻ cotransport activity than the previously reported fluorescent anion transporters.

MF, XW, DAM, AMG, WL and PAG acknowledge and pay respect to the Gadigal people of the Eora Nation, the traditional owners of the land on which we research, teach and collaborate at the University of Sydney. PAG thanks the Australian Research Council (DP200100453) and the University of Sydney for funding. MF thanks UOW for the University Postgraduate Award and International Postgraduate Tuition Award scholarships and the University of Sydney for funding.

Conflicts of interest

There are no conflicts to declare.

Notes and references

- [1] a) N. Mizushima, M. Komatsu, *Cell*, 2011, **147**, 728-741; b) D. C. Gadsby, *Nat. Rev. Mol. Cell Biol.*, 2009, **10**, 344-352.
- [2] a) A. S. Verkman, L. J. Galletta, *Nat. Rev. Drug Discov.*, 2009, **8**, 153; b) F. M. Ashcroft, *Ion channels and disease*, Academic Press, 1999; c) H. Li, H. Valkenier, L. W. Judd, P. R. Brotherhood, S. Hussain, J. A. Cooper, O. Jurcek, H. A. Sparkes, D. N. Sheppard, A. P. Davis, *Nat. Chem.*, 2016, **8**, 24-32.
- [3] J. B. Kim, *Korean J. Pediatr.*, 2014, **57**, 1-18.
- [4] J. M. Tomich, U. Bukovnik, J. Layman, B. D. Schultz, *Channel replacement therapy for cystic fibrosis*, IntechOpen, 2012.
- [5] a) N. Busschaert, S. H. Park, K. H. Baek, Y. P. Choi, J. Park, E. N. W. Howe, J. R. Hiscock, L. E. Karagiannidis, I. Marques, V. Felix, W. Namkung, J. L. Sessler, P. A. Gale, I. Shin, *Nat. Chem.*, 2017, **9**, 667-675; b) W. Van Rossom, D. J. Asby, A. Tavassoli, P. A. Gale, *Org. Biomol. Chem.*, 2016, **14**, 2645-2650; c) A. I. Share, K. Patel, C. Nativi, E. J. Cho, O. Francesconi, N. Busschaert, P. A. Gale, S. Roelens, J. L. Sessler, *Chem. Commun.*, 2016, **52**, 7560-7563; d) S. J. Moore, C. J. Haynes, J. González, J. L. Sutton, S. J. Brooks, M. E. Light, J. Herniman, G. J. Langley, V. Soto-Cerrato, R. Pérez-Tomás, *Chem. Sci.*, 2013, **4**, 103-117; e) L. E. Karagiannidis, C. J. Haynes, K. J. Holder, I. L. Kirby, S. J. Moore, N. J. Wells, P. A. Gale, *Chem. Commun.*, 2014, **50**, 12050-12053.
- [6] S. H. Park, S. H. Park, E. N. W. Howe, J. Y. Hyun, L. J. Chen, I. Hwang, G. Vargas-Zuniga, N. Busschaert, P. A. Gale, J. L. Sessler, I. Shin, *Chem*, 2019, **5**, 2079-2098.
- [7] V. Soto-Cerrato, P. Manuel-Manresa, E. Hernando, S. Calabuig-Farinas, A. Martinez-Romero, V. Fernandez-Duenas, K. Sahlholm, T. Knopf, M. Garcia-Valverde, A. M. Rodilla, E. Jantus-Lewintre, R. Farras, F. Ciruela, R. Perez-Tomas, R. Quesada, *J. Am. Chem. Soc.*, 2015, **137**, 15892-15898.
- [8] S. N. Berry, V. Soto-Cerrato, E. N. Howe, H. J. Clarke, I. Mistry, A. Tavassoli, Y.-T. Chang, R. Pérez-Tomás, P. A. Gale, *Chem. Sci.*, 2016, **7**, 5069-5077.
- [9] X. Wu, E. N. W. Howe, P. A. Gale, *Acc. Chem. Res.*, 2018, **51**, 1870-1879.
- [10] X. Bao, X. Wu, S. N. Berry, E. N. W. Howe, Y. T. Chang, P. A. Gale, *Chem. Commun.*, 2018, **54**, 1363-1366.
- [11] a) S. J. Brooks, P. R. Edwards, P. A. Gale, M. E. Light, *New J. Chem.*, 2006, **30**, 65-70; b) C. M. Dias, H. Y. Li, H. Valkenier, L. E. Karagiannidis, P. A. Gale, D. N. Sheppard, A. P. Davis, *Org. Biomol. Chem.*, 2018, **16**, 1083-1087.
- [12] R. L. Atkins, D. E. Bliss, *J. Org. Chem.*, 1978, **43**, 1975-1980.
- [13] T. S. Reddy, A. R. Reddy, *Dyes Pigm.*, 2013, **96**, 525-534.
- [14] E. N. Howe, N. Busschaert, X. Wu, S. N. Berry, J. Ho, M. E. Light, D. D. Czech, H. A. Klein, J. A. Kitchen, P. A. Gale, *J. Am. Chem. Soc.*, 2016, **138**, 8301-8308.
- [15] S. Bhosale, S. Matile, *Chirality*, 2006, **18**, 849-856.
- [16] X. Wu, J. R. Small, A. Cataldo, A. M. Withecombe, P. Turner, P. A. Gale, *Angew. Chem. Int. Ed. Engl.*, 2019, **58**, 15142-15147.

Supporting Information
for
Coumarin-bisureas as potent fluorescent
transmembrane anion transporters

Mohamed Fares,^{a-c} Xin Wu,^a Daniel A. McNaughton,^a Alexander Gilchrist,^a William Lewis,^a Paul A. Keller,^b Alain Arias-Betancur^{d,e}, Ricardo Pérez-Tomás^d, Philip A. Gale,^{*a,f}

- a. School of Chemistry, The University of Sydney, NSW 2006, Australia E-mail: philip.gale@sydney.edu.au
- b. School of Chemistry & Molecular Bioscience, Molecular Horizons, University of Wollongong, and Illawarra Health & Medical Research Institute, Wollongong, NSW 2522, Australia.
- c. Department of Pharmaceutical Chemistry, Faculty of Pharmacy, Egyptian Russian University, Cairo 11829, Egypt
- d. Department of Pathology and Experimental Therapeutics, Faculty of Medicine and Health Sciences, Universitat de Barcelona, 08905 Barcelona, Spain
- e. Department of Integral Adult Dentistry, Research Centre for Dental Sciences (CICO), Universidad de La Frontera, Temuco 4811230, Chile
- f. The University of Sydney Nano Institute (SydneyNano), The University of Sydney, NSW 2006, Australia.

Table of Contents

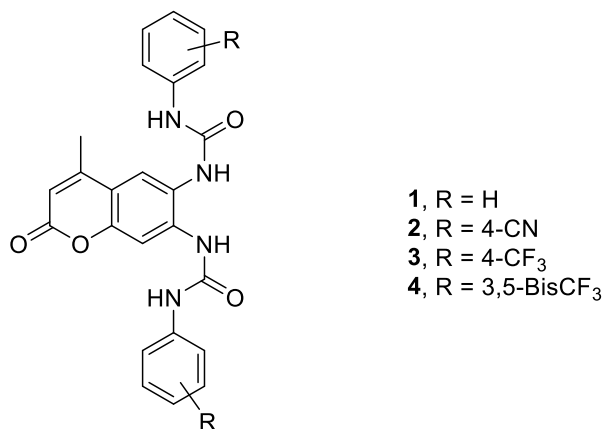
S1. General methods and material	2
S2. Synthesis and characterization:	3
S2.1. Overview of compounds:	3
S2.2. Synthetic strategy of target anion transporters 1-4	3
S3. ¹H NMR and ¹³C NMR Data	9
S4. X-ray Crystallography:	22
S5. ¹H NMR Titration Binding Studies with TBACl	24
S6. Anion Transport Studies	29
S6.1: Ion selective electrode (ISE) assays:	29
S6.2: General preparation for HPTS assays:	37
S7. Biological results:	47
7.1 Cell viability assay (MTT)	47
S8. References:	48

S1. General methods and material

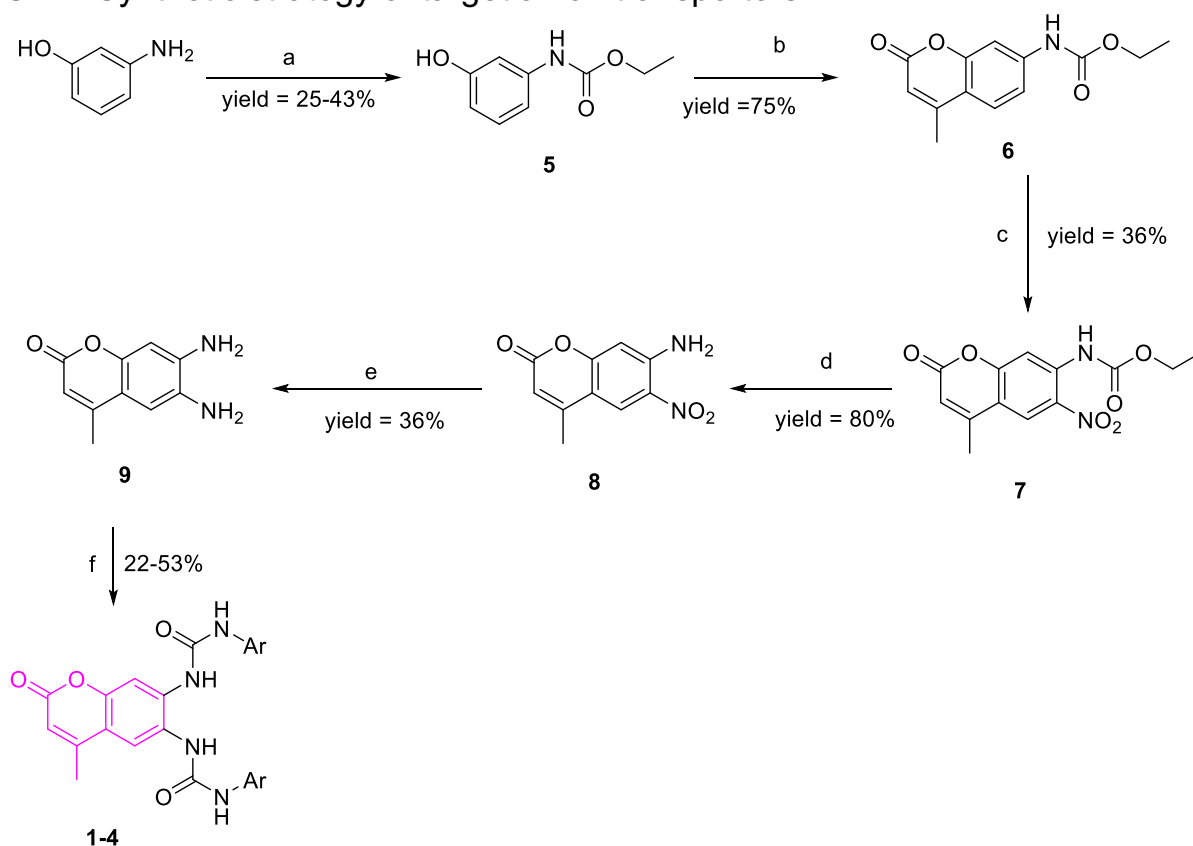
All reagents and solvents were purified and dried by standard techniques. Reactions were monitored by TLC analysis using silica gel GF/UV 254. NMR spectra were recorded on Bruker 400 MHz FT-NMR spectrometer and Varian Gemini-300BB 300 MHz FT-NMR spectrometers (Varian Inc., Palo Alto, CA). ^1H spectra were run at 300 and 400 MHz and ^{13}C spectra were run at 75 and 101 MHz, in the stated solvent. Chemical shifts (δ_{H}) are reported relative to TMS as internal standard and coupling constant (J) values are reported in Hertz. The abbreviations used are as follows: s, singlet; d, doublet; t, triplet; m, multiplet. Electrospray (ESI single quadrupole) mass spectra have their ion mass to charge values (m/z) stated with their relative abundances as a percentage in parentheses. Peaks assigned to the molecular ion are denoted as $[\text{M}+\text{H}]$ or $[\text{M}+\text{Na}]$. Column chromatography was performed using silica gel 60 (0.063-0.200 mm). Low resolution mass spectra (LRMS) and high resolution mass spectra (HRMS) were recorded using positive/negative ion electrospray ionization (ESI) on Bruker amaZon SL mass spectrometer.

S2. Synthesis and characterization:

S2.1. Overview of compounds:

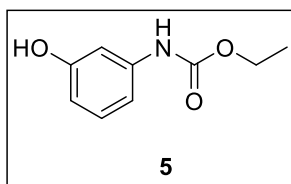


S2.2. Synthetic strategy of target anion transporters 1-4



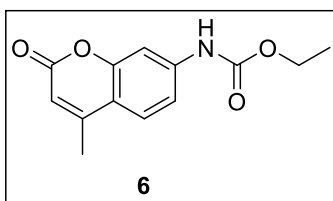
Scheme 1. a- Ethylchloroformate/DEE; b-Ethylacetoacetate, 70% H₂SO₄; c- Al(NO₃)₃·9 H₂O, acetic anhydride; d- Conc H₂SO₄, Glacial acetic acid, reflux.; e- Sn/HCl, reflux.; f- Suitable isocyanate, DCM, 45 °C, or Suitable isocyanate, 45 °C.

Synthesis of ethyl (3-hydroxyphenyl)carbamate **5**:¹ To a suspension of *m*-aminophenol



(10.0 g, 92.0 mmol) in diethyl ether (400 mL), ethyl chloroformate (10.0 g, 92.0 mmol) was added at once and a white precipitate appeared immediately. The reaction mixture was stirred for 2 h and the resulting salt was removed by filtration, while the solvent was removed under vacuum to give 8 g of white solid which was used in the next step without any further purification.¹

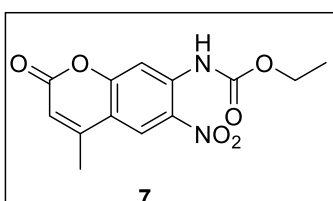
Synthesis of ethyl(4-methyl-2-oxo-2*H*-chromen-7-yl)carbamate **6**:¹ To a mixture of ethyl



(3-hydroxyphenyl)carbamate **5** (8.0 g, 44.0 mmol) and ethylacetoacetate (6.8 mL, 53.0 mmol), 100 mL of 70% H₂SO₄ was added. The reaction mixture was stirred for 4 h at room temperature. The resulting solid was collected by

filtration, washed with water (2 x 30 mL) and recrystallized from ethanol to give **6** (8.2 g, 75%) as a colorless needles. ¹H NMR (400 MHz, DMSO-*d*₆) δ: 1.40 (t, *J* = 7.0 Hz, 3H, CH₂CH₃), 2.50 (s, 3H, CH₃), 4.31 (q, *J* = 7.0 Hz, 2H, CH₂CH₃), 6.32 (s, 1H, ArH), 7.51 (dd, *J* = 2.0, 9.0 Hz, 1H, ArH), 7.65 (d, *J* = 2.0 Hz, 1H, ArH), 7.77 (d, *J* = 9.0 Hz, 1H, ArH), 10.24 (s, 1H, NH); ¹³C NMR (101 MHz, DMSO-*d*₆) δ: 14.9, 18.4, 61.1, 104.8, 112.3, 114.6, 114.7, 126.3, 143.3, 153.6, 153.8, 154.3, 160.5.

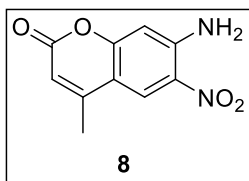
Synthesis of ethyl (4-methyl-6-nitro-2-oxo-2*H*-chromen-7-yl)carbamate **7**:² To a



suspension of 7-carbethoxyamino-4-methylcoumarin **6** (4.1 g, 16.6 mmol) in acetic anhydride (100 mL), aluminium nitrate nonahydrate (5.6 g, 6.5 mmol) was added portionwise and the reaction mixture was stirred for 16 h. The mixture was slowly poured into ice cold water (200 mL) and the resulting

yellow residue was purified *via* flash chromatography (hexane: ethyl acetate = 9:1) to give **7** (1.7 g, 36%). ¹H NMR (500 MHz, DMSO-*d*₆) δ: 1.27 (t, *J* = 7.0 Hz, 3H, CH₂CH₃), 2.45 (s, 3H, CH₃), 4.18 (q, *J* = 7.0 Hz, 2H, CH₂CH₃), 6.46 (s, 1H, ArH), 7.72 (s, 1H, ArH), 8.35 (s, 1H, ArH), 10.10 (s, 1H, NH); ¹³C NMR (126 MHz, DMSO-*d*₆) δ: 14.7, 18.3, 62.2, 109.9, 114.9, 115.7, 123.9, 136.1, 136.9, 152.8, 153.5, 156.3, 159.3; LRMS ESI⁻ (*m/z*): 291 (100%, M-H)⁻.

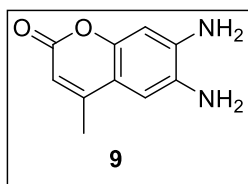
Synthesis of 7-Amino-4-methyl-6-nitro-2*H*-chromen-2-one **8**:² 6-Nitro-7-



carbethoxyamino-4-methylcoumarin **7** (1.7 g, 5.8 mmol) was heated at reflux in a mixture of concentrated sulfuric acid (6 g) and glacial acetic acid (6 g) for 4 h. After cooling the reaction mixture, was poured into ice water (30 mL) and let stand overnight. Ice was

added, and neutralization of the acidic solution was accomplished using NaOH (50%). The formed yellow precipitate was filtered, washed thoroughly 3 times with ice water (3 x 10 mL) and dried to give **8** as a yellow powder (1.0 g, 80%). **¹H NMR (400 MHz, DMSO-*d*₆)** δ : 2.38 (s, 3H, CH₃), 6.18 (s, 1H, ArH), 6.81 (s, 1H, ArH), 7.80 (br. s, 2H, NH₂), 8.33 (s, 1H, ArH); **¹³C NMR (101 MHz, DMSO-*d*₆)** δ : 18.2, 103.3, 110.4, 111.6, 124.9, 128.8, 148.6, 153.4, 157.6, 159.7. **LRMS ESI⁻ (*m/z*)**: 219 (100%, M-H)⁻.

Synthesis of 6,7-Diamino-4-methyl-2*H*-chromen-2-one **9**:² Conc. hydrochloric acid (15



mL) was added in three portions over 20 minutes to a mixture of tin powder (1.1 g, 9.2 mmol) and 6-nitro-7-amino-4-methyl-coumarin (1 g, 4.5 mmol) and the reaction mixture was heated at reflux for 3 h. After cooling, the reaction mixture was poured into ice water (50 mL)

and let stand overnight. Ice was added, and neutralization of the acidic solution was accomplished using NaOH (50%). The formed precipitate was extracted with ethyl acetate (3 x 200 mL) and all the organic layers washed with water (2 x 10 mL), brine (1 x 10 mL) and dried over magnesium sulfate. Ethyl acetate was removed under vacuum to give **9** as a dark yellow powder (0.31 g, 36%). **¹H NMR (300 MHz, DMSO-*d*₆)** δ : 2.26 (s, 3H, CH₃), 4.72 (br. s, 2H, NH₂), 5.63 (br. s, 2H, NH₂), 5.87 (s, 1H, ArH), 6.44 (s, 1H, ArH), 6.76 (s, 1H, ArH); **¹³C NMR (75 MHz, DMSO-*d*₆)** δ : 18.1, 99.0, 107.1, 107.6, 109.2, 131.9, 141.3, 148.1, 153.1, 161.1. **LRMS ESI⁻ (*m/z*)**: 191 (100%, M-H)⁻. **HRMS (ESI⁺)** calcd for C₁₀H₁₀N₂NaO₂ (M + Na⁺): 213.0635, found: 213.06340 (0.22 ppm).

Synthesis of target compounds **1-4**:

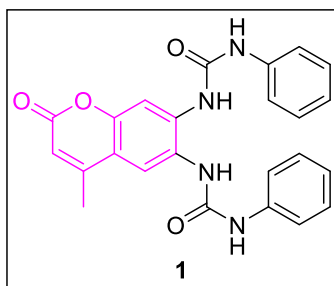
General procedure A:

6,7-Diamino-4-methylcoumarin **9** (80 mg, 0.42 mmol) was suspended in CH₂Cl₂ and added dropwise to the corresponding isocyanate derivative solution with stirring. The suspension was stirred at 45 °C overnight and after cooling the solvent removed under vacuum. The resulting residue was heated in ethanol (25 mL) and filtered while hot to give anion transporters **1**, **2** and **4**.

Procedure B:

Under inert atmosphere, 4-trifluoromethylphenyl isocyanate (0.79 g, 4.2 mmol) was added to 6,7-diamino-4-methylcoumarin **9** (80 mg, 0.42 mmol) with constant stirring. The reaction mixture was held at 45 °C overnight and after cooling the unreacted 4-trifluoromethylphenyl isocyanate was removed under vacuum and the remaining residue was heated in ethanol (25 mL) and filtered while hot to give **3** as white solid.

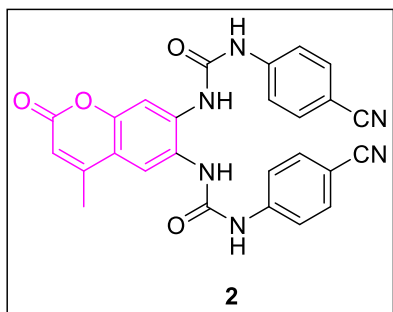
1,1'-(4-Methyl-2-oxo-2*H*-chromene-6,7-diyl)bis(3-phenylurea) **1**: Using the general



procedure A and phenyl isocyanate (200 mg, 1.68 mmol), compound **1** (70 mg, 39%) was isolated as a white solid. **¹H NMR (400 MHz, DMF-*d*₇)** δ : 2.40 (s, 3H, CH₃), 6.22 (s, 1H, ArH), 6.97 (q, *J* = 7.0 Hz, 2H, ArH), 7.27 (t, *J* = 7.0 Hz, 4H, ArH), 7.54 (m, 4H, ArH) 7.79 (s, 1H, ArH), 8.07 (s, 1H, ArH),

8.18 (s, 1H, NH), 8.68 (s, 1H, NH), 9.06 (s, 1H, NH), 9.46 (s, 1H, NH); **¹³C NMR (101 MHz, DMF-*d*₇)** δ : 17.8, 107.3, 112.6, 114.6, 118.5, 118.7, 122.1, 122.5, 123.3, 125.2, 129.0, 129.1, 139.5, 140.1, 140.7, 152.1, 152.9, 153.2, 160.6. **LRMS ESI⁻ (*m/z*):** 427 (100%, M-H)⁻. **HRMS (ESI⁻)** calcd for C₂₄H₁₉N₄O₄ (M-H)⁻: 427.1412, found: 427.1412 (-0.06 ppm).

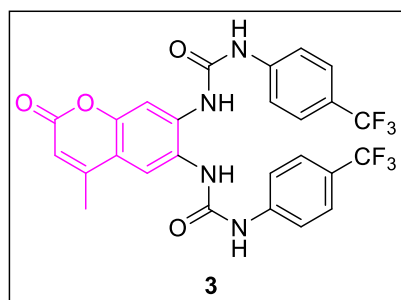
1,1'-(4-Methyl-2-oxo-2H-chromene-6,7-diyl)bis(3-(4-cyanophenyl)urea) **2**: Using the



general procedure A and *p*-cyanophenyl isocyanate (242 mg, 1.68 mmol), compound **2** (106 mg, 53%) was isolated as a buff solid. **¹H NMR (500 MHz, DMSO-*d*₆) δ**: 2.39 (s, 3H, CH₃), 6.29 (s, 1H, ArH), 7.64-7.77 (m, 9H, ArH), 8.02 (s, 1H, ArH), 8.25 (s, 1H, NH), 8.65 (s, 1H, NH), 9.57 (s, 1H, NH), 9.91 (s, 1H, NH); **¹³C NMR (126 MHz, DMSO-*d*₆) δ**: 18.5, 103.8, 104.2, 107.7, 113.1,

114.9, 118.6, 118.7, 119.7, 119.8, 123.7, 124.7, 133.8, 133.9, 138.5, 144.1, 144.8, 151.7, 152.4, 153.4, 154.0, 160.0. **LRMS ESI⁻ (*m/z*)**: 513 (100%, M+Cl)⁻. **HRMS (ESI⁺)** calcd for C₂₆H₁₈N₆O₄Na (M+Na)⁺: 501.1282, found: 501.1287 (1.0 ppm).

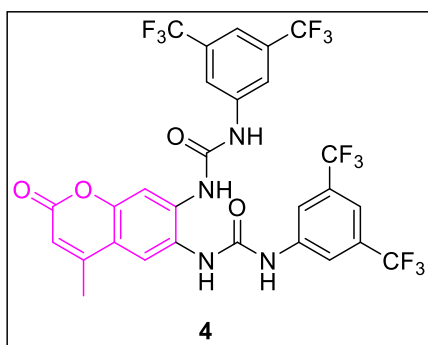
1,1'-(4-Methyl-2-oxo-2H-chromene-6,7-diyl)bis(3-(4-(trifluoromethyl)phenyl)urea) **3**:



Using the procedure B and *p*-trifluoromethylphenyl isocyanate (0.79 g, 4.2 mmol), compound **3** (53 mg, 22%) was isolated as a white solid. **¹H NMR (400 MHz, DMF-*d*₇) δ**: 2.64 (s, 3H, CH₃), 6.48 (s, 1H, ArH), 7.87 (d, *J* = 9.0 Hz, 4H, ArH), 7.95-8.05 (m, 4H, ArH), 8.21 (s, 1H, ArH), 8.40 (s, 1H, ArH), 8.51 (s, 1H, NH), 9.03 (s, 1H, NH), 9.79 (s, 1H, NH), 10.06 (s, 1H, NH); **¹³C NMR**

(101 MHz, DMF-*d*₇) δ: 17.8, 107.6, 112.9, 115.0, 118.4, 118.5, 122.6, 122.9, 123.0, 123.3, 123.5, 123.7, 125.0, 126.4, 139.0, 143.7, 144.3, 152.1, 152.7, 153.2, 154.3, 160.5; **¹⁹F** (376 MHz, DMF-*d*₇) δ: -60.03, -60.15. **LRMS ESI⁻ (*m/z*)**: 563 (100%, M-H)⁻. **HRMS (ESI⁻)** calcd for C₂₆H₁₇F₆N₄O₄ (M-H)⁻: 563.1160, found: 563.1160 (-0.10 ppm).

1,1'-(4-Methyl-2-oxo-2H-chromene-6,7-diyl)bis(3-(3,5-bis(trifluoromethyl)phenyl)urea) **4**:

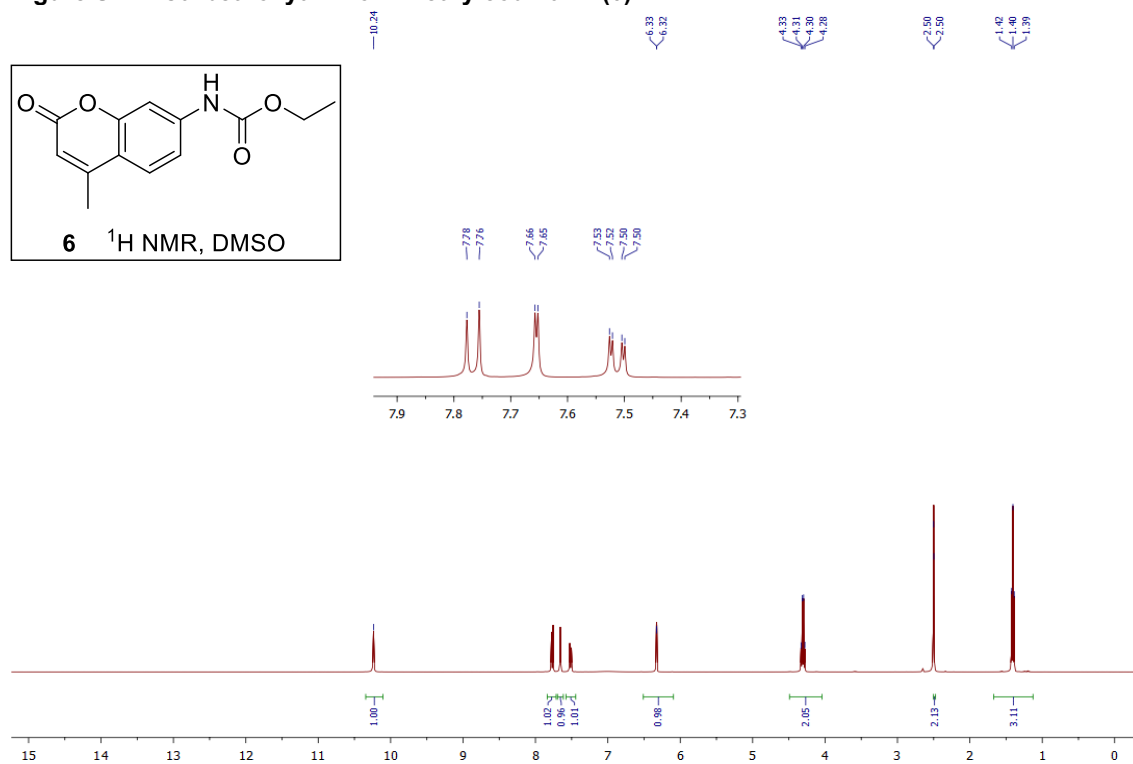


Using the general procedure A and *p*-cyanophenyl isocyanate (428 mg, 1.68 mmol), compound **4** (78 mg, 27%) was isolated as a buff solid. **¹H NMR (400 MHz, DMF-*d*₇) δ**: 2.49 (s, 3H, CH₃), 6.31 (s, 1H, ArH), 7.68 (s, 1H, ArH), 7.71 (s, 1H, ArH), 8.05 (d, *J* = 7.0 Hz, 4H, ArH), 8.23-8.26 (m, 4H, ArH), 8.99 (s, 1H, NH), 9.41 (s, 1H, NH), 10.54 (s, 1H, NH), 10.80 (s, 1H,

NH); **¹³C NMR (101 MHz, DMF-*d*₇) δ**: 17.7, 107.1, 112.8, 114.7, 117.8, 119.7, 121.6, 122.4, 122.4, 124.5, 125.1, 127.8, 127.8, 131.4, 137.1, 142.1, 142.7, 151.4, 152.6, 153.1, 153.8, 160.3; **¹⁹F (376 MHz, DMF-*d*₇) δ**: -61.36, -61.44. **LRMS ESI⁺ (*m/z*)**: 723 (100%, M+Na)⁺. **HRMS (ESI⁺)** calcd for C₂₈H₁₆F₁₂N₄O₄Na (M+Na)⁺: 723.0872, found: 723.0875 (0.4 ppm).

S3. ^1H NMR and ^{13}C NMR Data

Figure S1: 7-Carboethoxyamino-4-methylcoumarin (6)



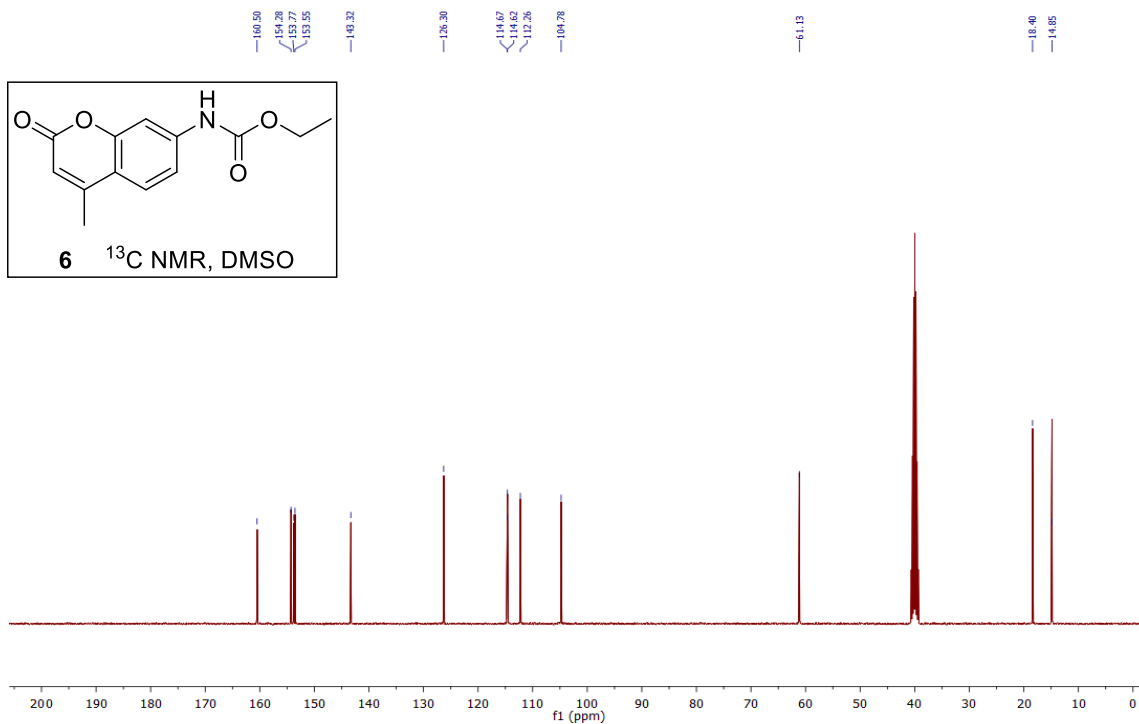
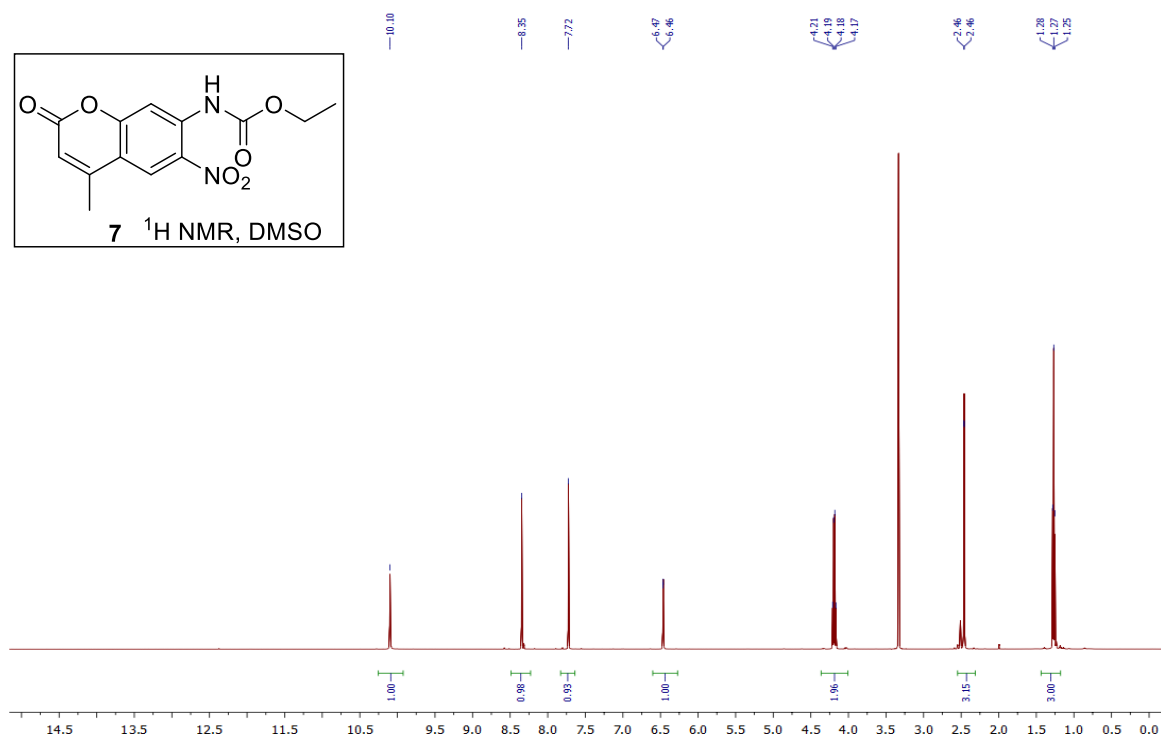
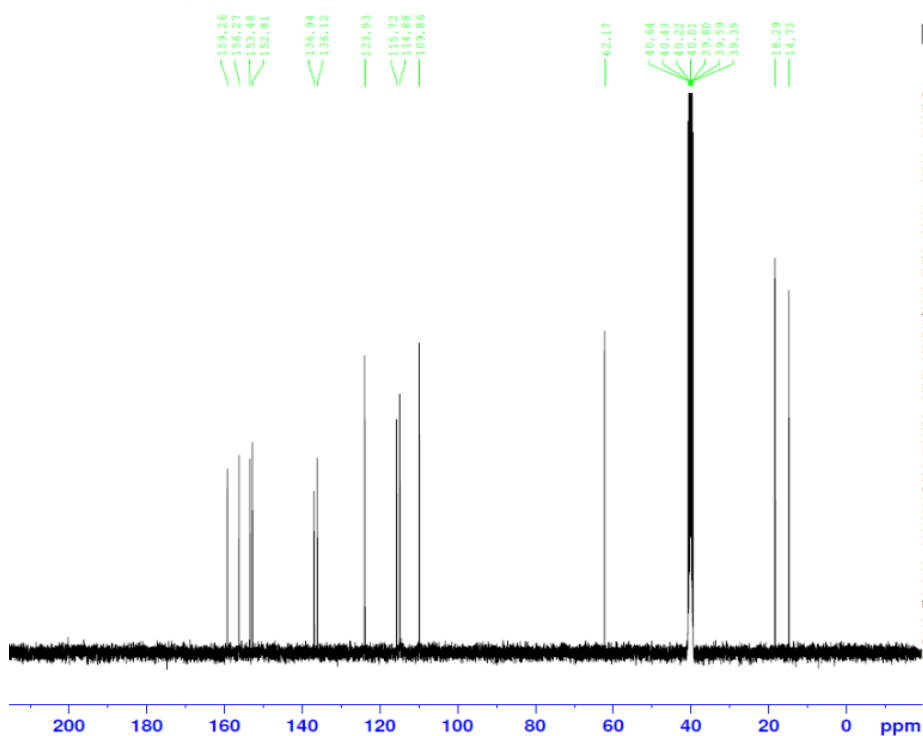
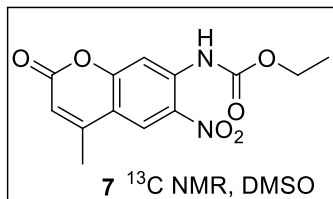


Figure S2: 6-Nitro-7- carbethoxyamino-4-methylcoumarin (7)





```

Current Data Parameters
NAME      mfm_181017_34
EXPNO    2
PROCNO   1

F2 - Acquisition Parameters
Date_    20181018
Time     3.02 h
INSTRUM  spect
PROBHD   z108618_0921 (
PULPROG  zgpg30
TD        65536
SOLVENT  DMSO
NS        1024
DS         4
SWH       24038.461 Hz
FIDRES    0.733596 Hz
AQ         1.3631488 sec
RG         196.38
DW         20.800 usec
DE         6.50 usec
TE         299.1 K
D1         2.0000000 sec
D11        0.0300000 sec
TD0        1
SFO1      100.6303741 MHz
NUC1       13C
P1         10.00 usec
PLW1      55.50099945 W
SFO2      400.1616006 MHz
NUC2       1H
CPDPRG[2  waltz16
PCPD2     90.00 usec
PLW2     11.52400017 W
PLW12    0.27886000 W
PLW13    0.14026000 W

F2 - Processing parameters
SI         32768
SF         100.6203120 MHz
WDW        EM
SSB        0
LB         1.00 Hz
GB         0
PC         1.40
  
```

Figure S3: 6-Nitro-7-amino-4-methylcoumarin (**8**)

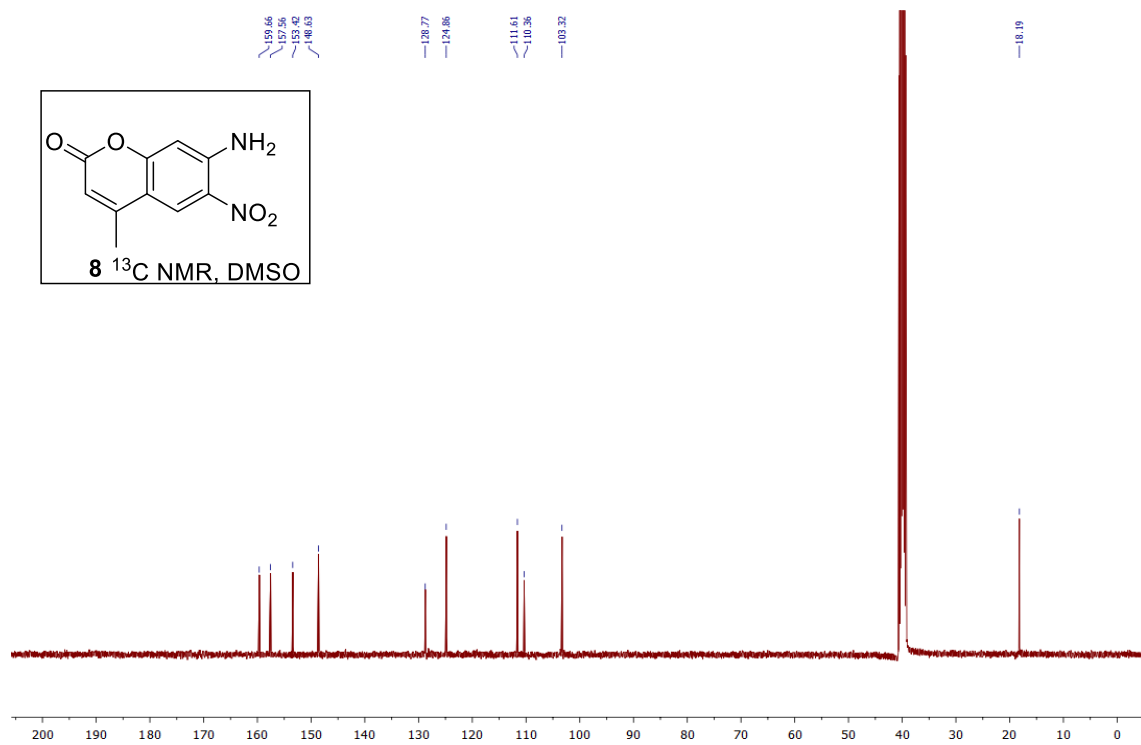
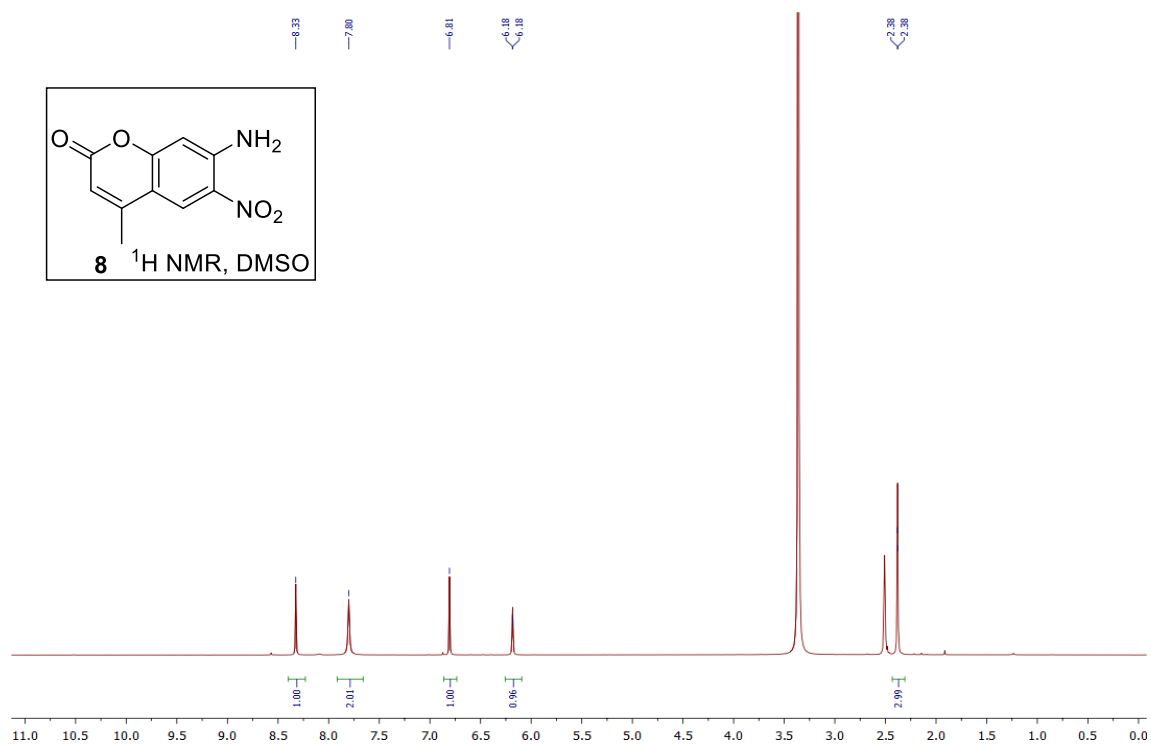


Figure S4: 6,7-Diamino-4-methylcoumarin (9)

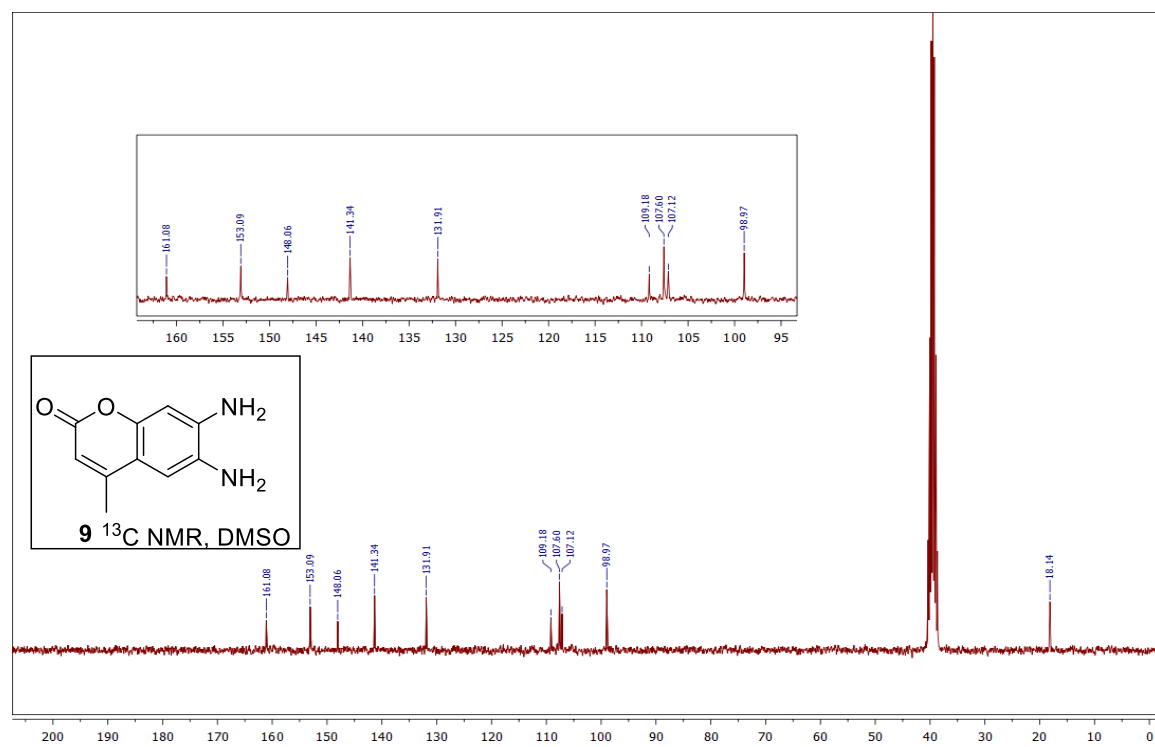
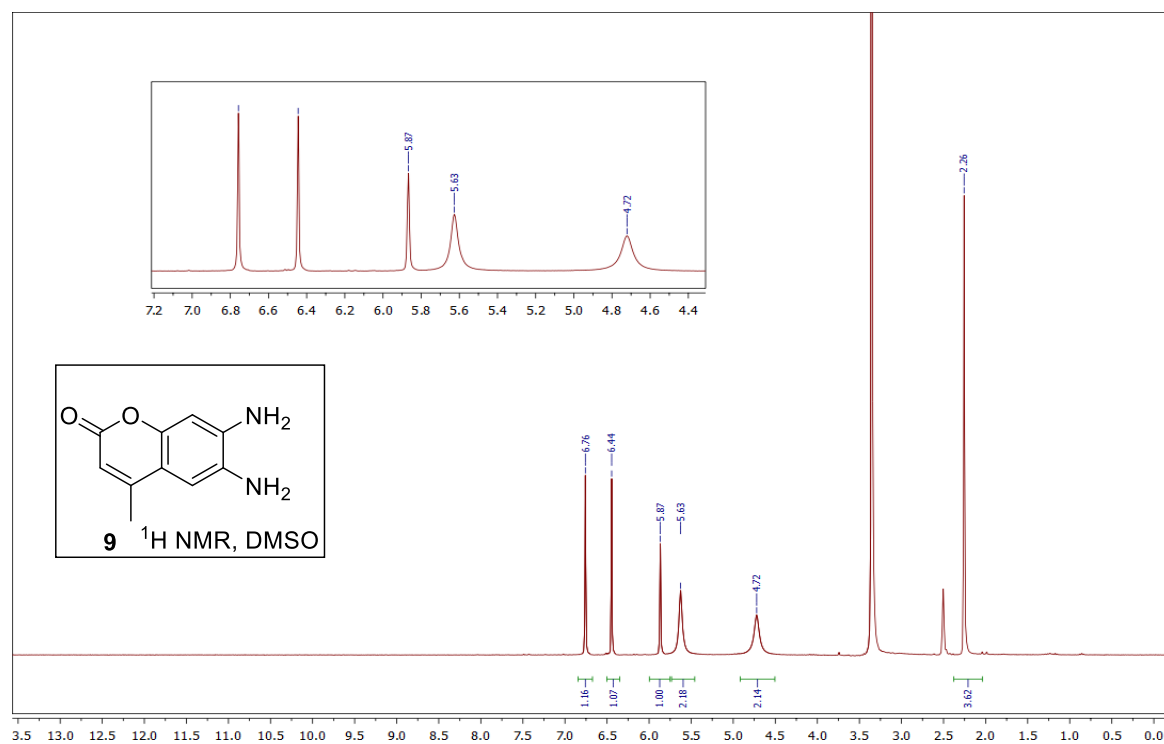
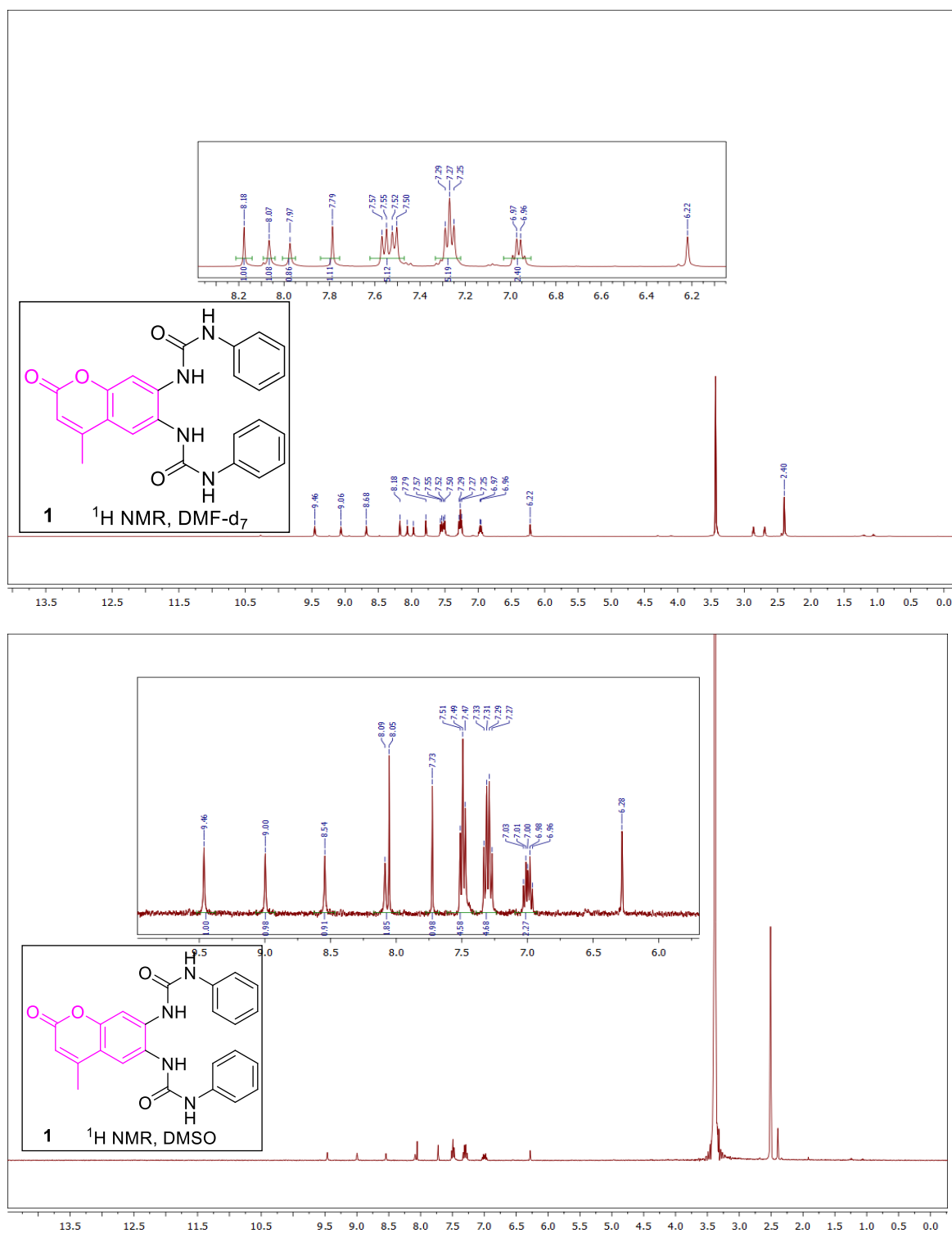


Figure S5: 1,1'-(4-methyl-2-oxo-2H-chromene-6,7-diyl)bis(3-phenylurea) (1)



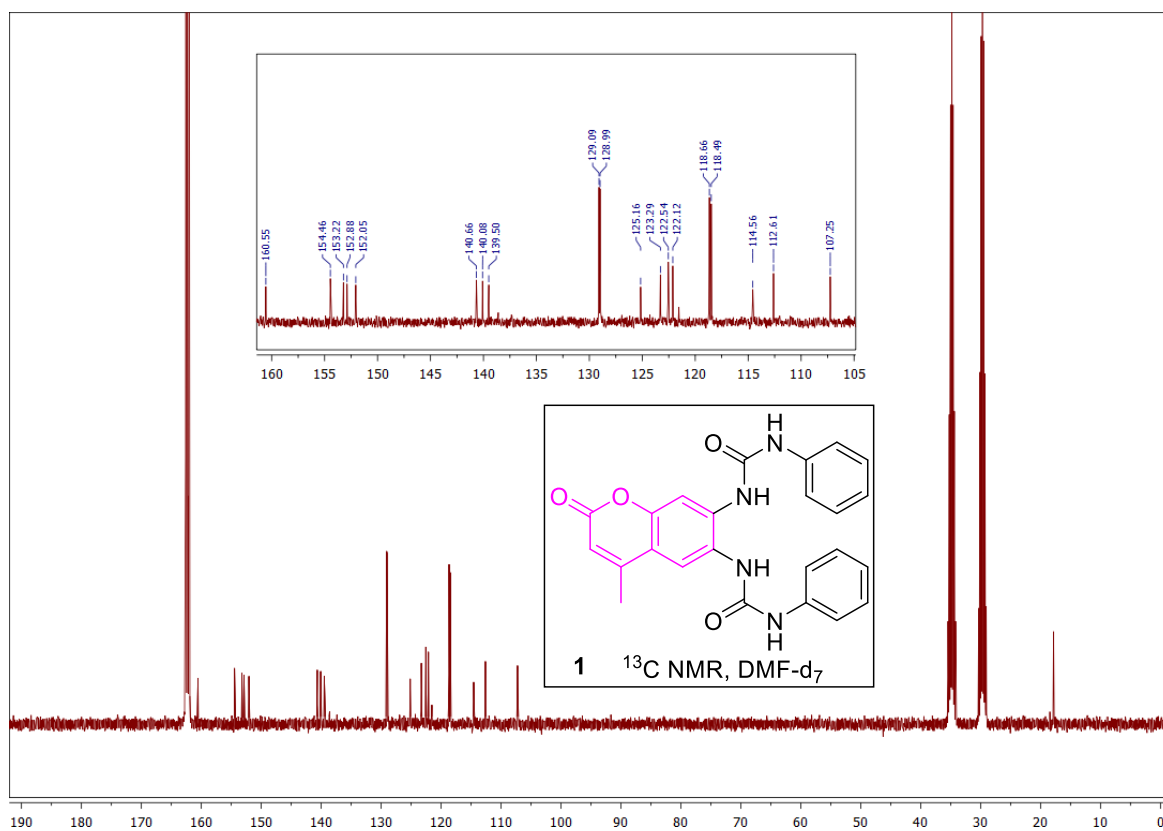
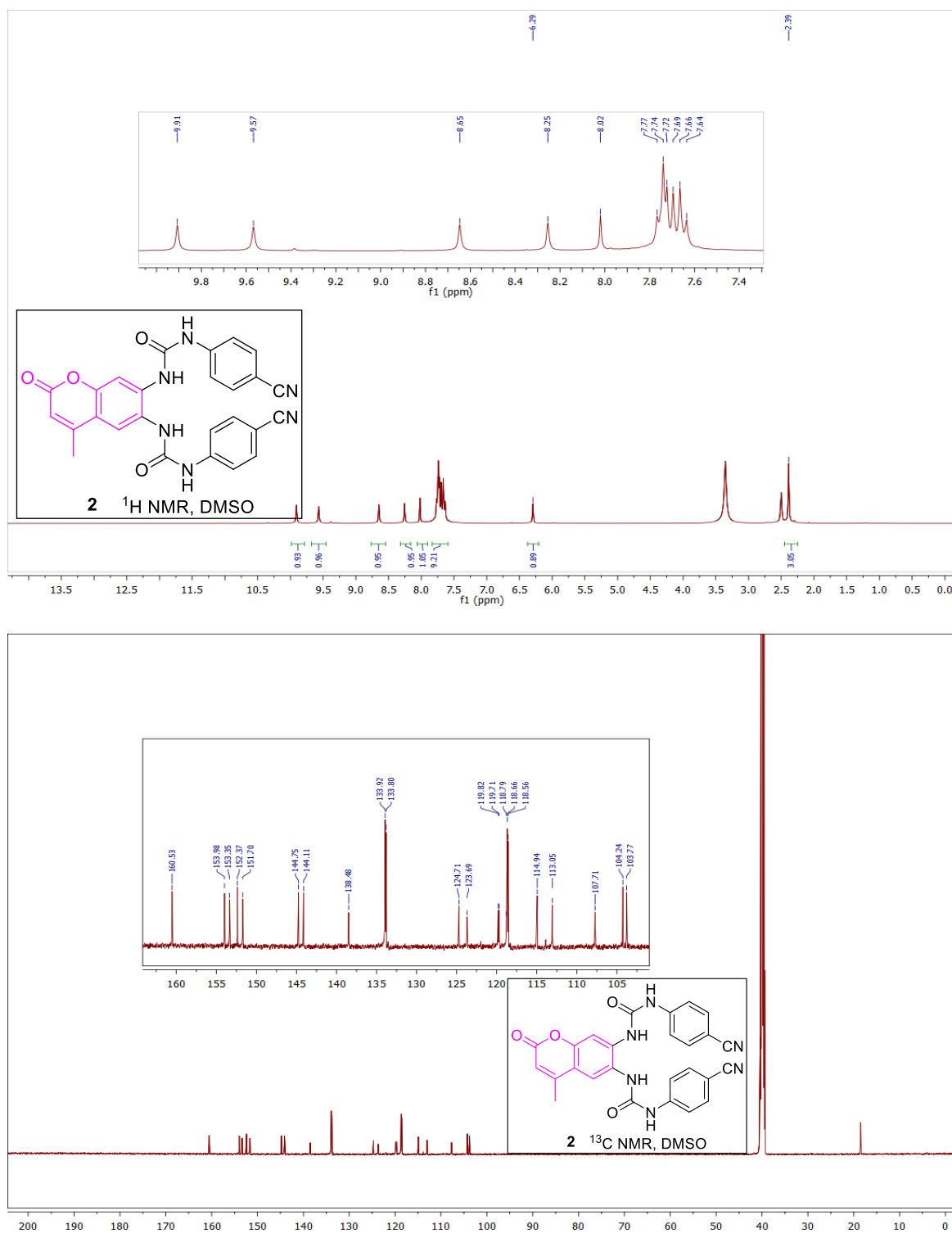


Figure S6: 1,1'-(4-methyl-2-oxo-2H-chromene-6,7-diyl)bis(3-(4-cyanophenyl)urea) (2)



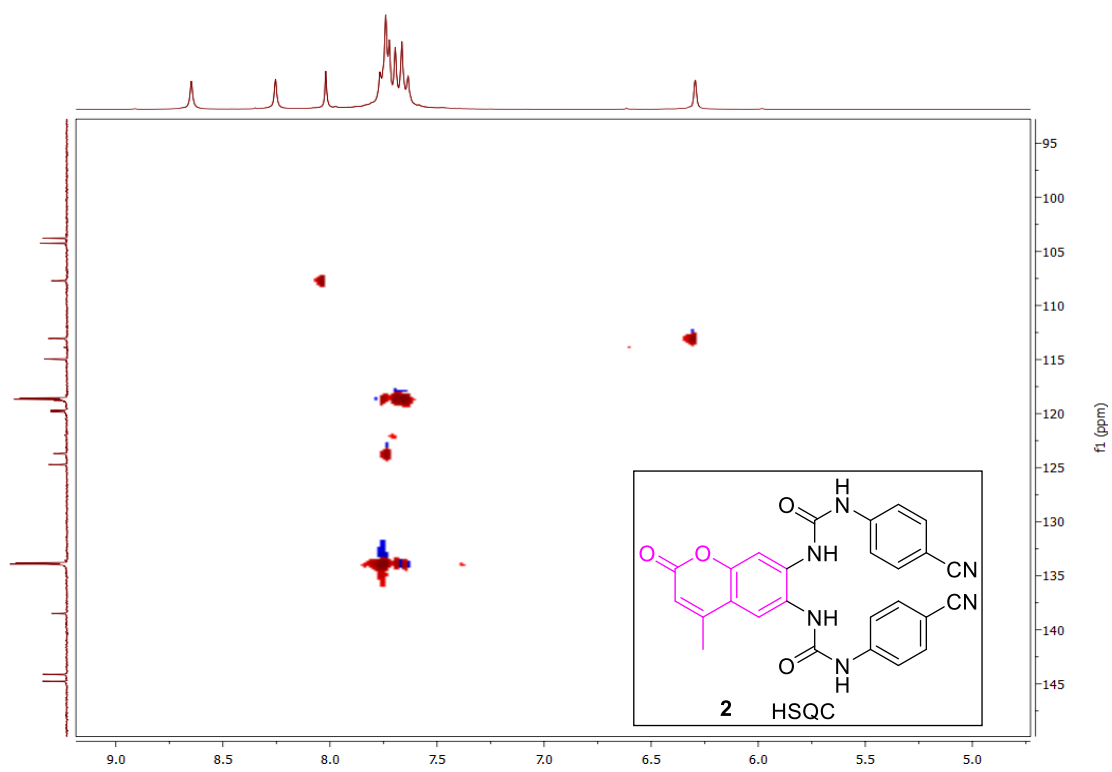
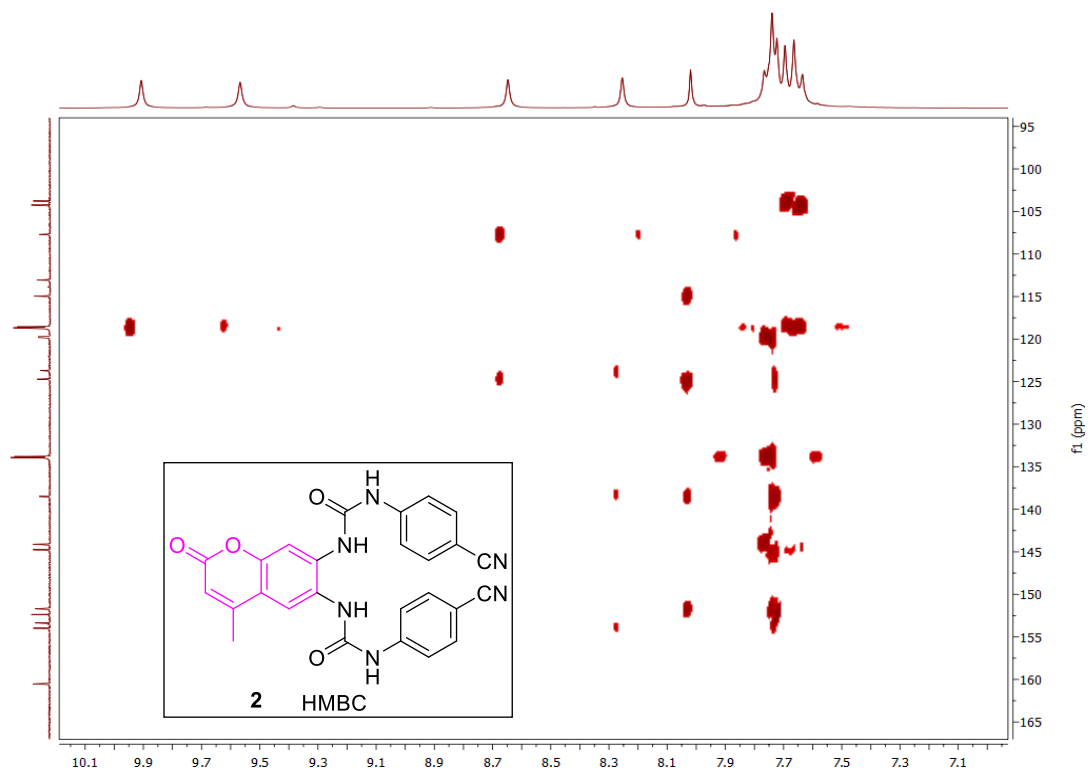
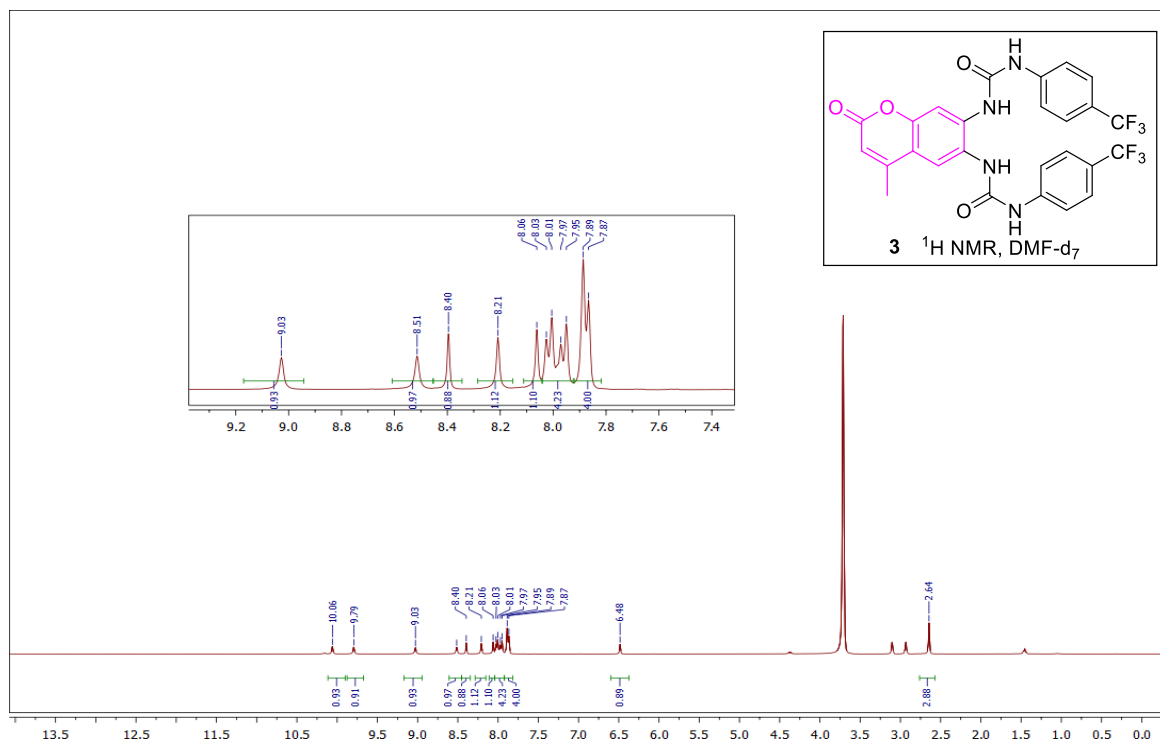
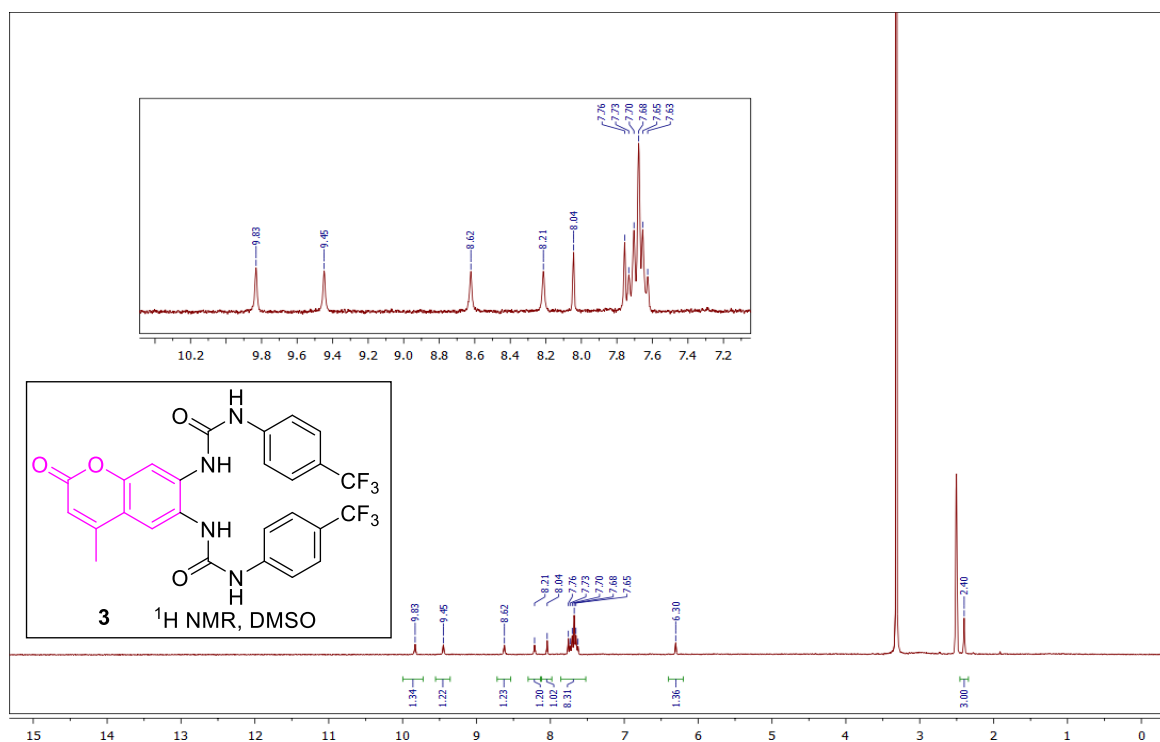


Figure S7: 1,1'-(4-methyl-2-oxo-2H-chromene-6,7-diyl)bis(3-(4-(trifluoromethyl)phenyl)urea) (3)



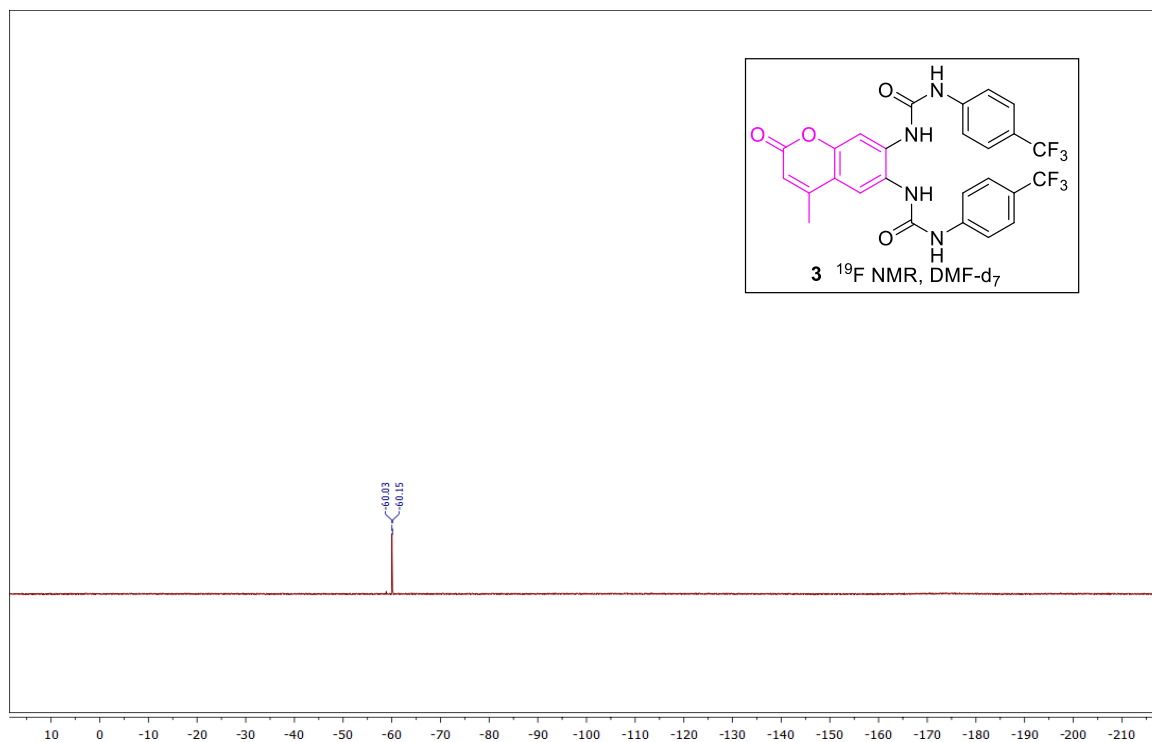
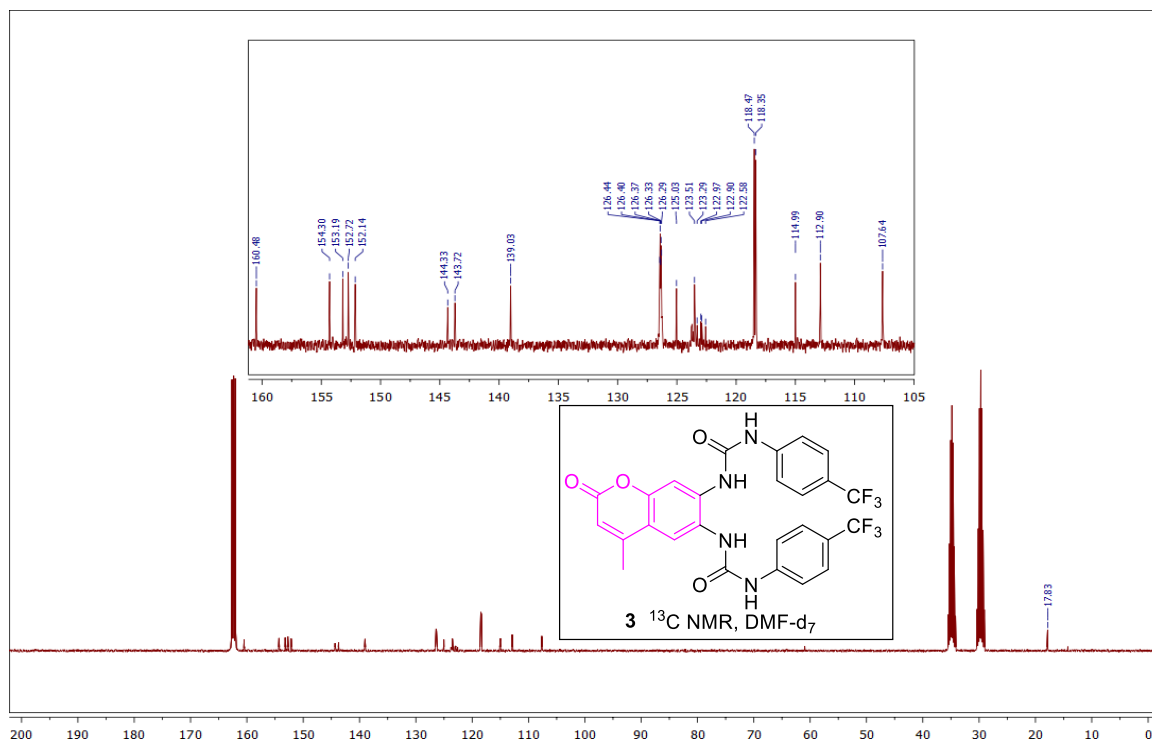
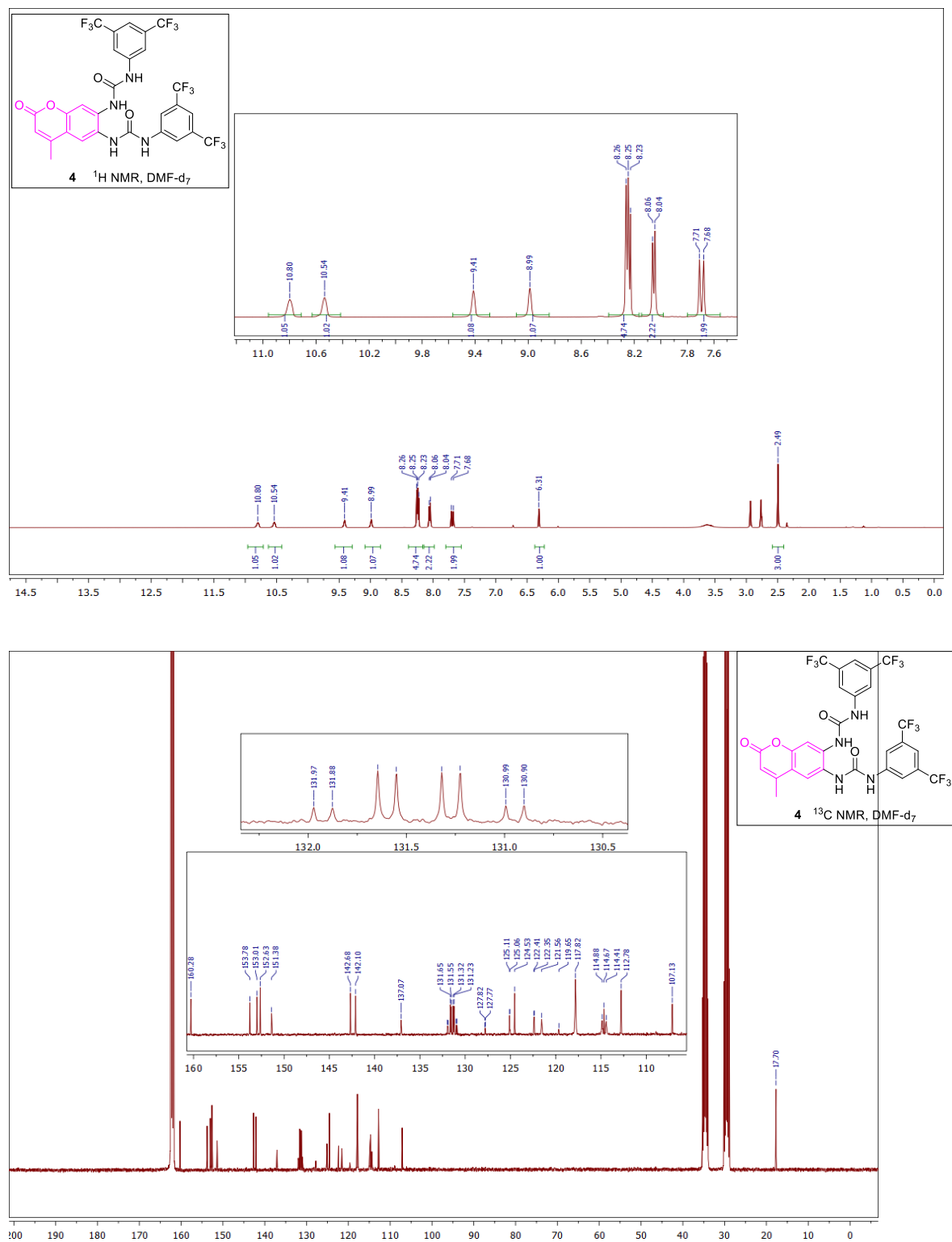
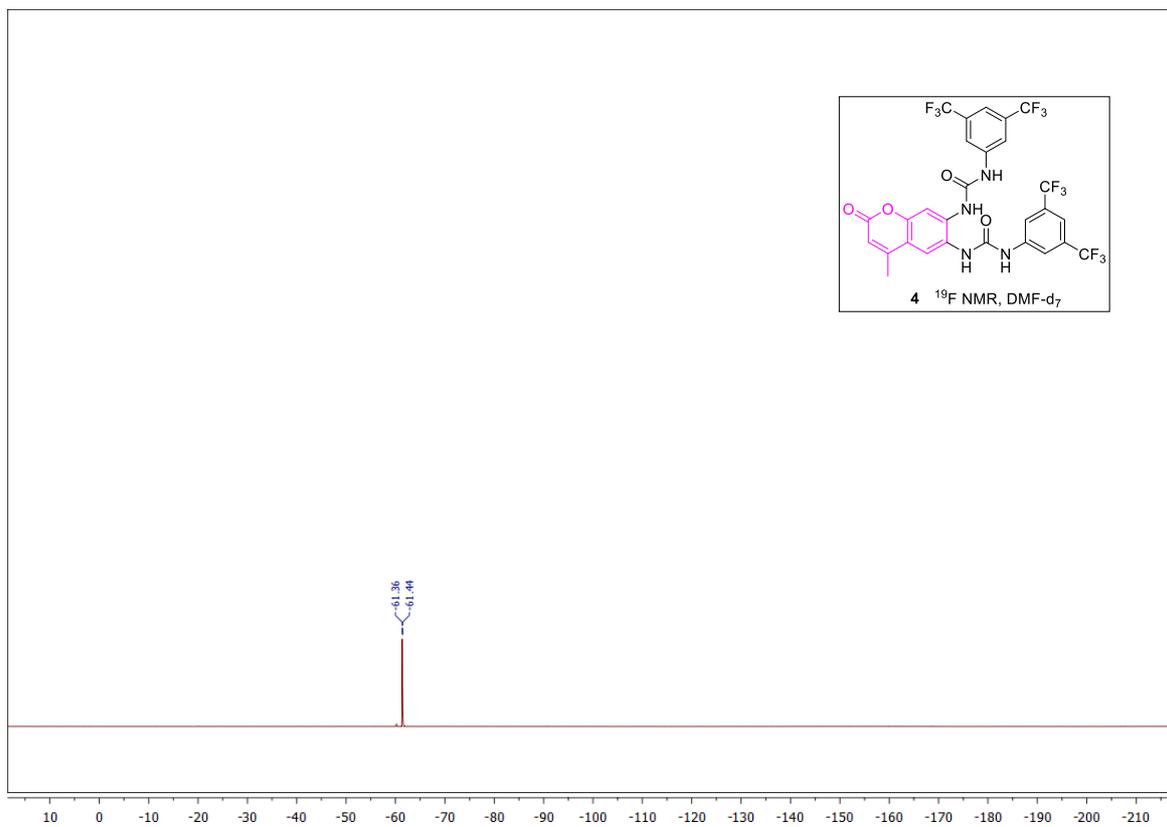


Figure S8: 1,1'-(4-methyl-2-oxo-2H-chromene-6,7-diyl)bis(3-(3,5-bis(trifluoromethyl)phenyl)urea) (4)





S4. X-ray Crystallography:

S5.1. X-ray of complex 1

Single crystals of transporter **1** $C_{26}H_{26}N_4O_5$ were crystallised from a mixture of dimethylformamide and ethanol. A suitable crystal was selected and in Paratone on a micromount on a SuperNova, Dual, Cu at home/near, Atlas diffractometer. The crystal was kept at 100 K during data collection. Using Olex2³, the structure was solved with the ShelXS⁴ structure solution program using Direct Methods and refined with the ShelXL⁵ refinement package using Least Squares minimization.

Crystal Data for $C_{26}H_{26}N_4O_5$ ($M=474.51$ g/mol): monoclinic, space group P2/c (no. 13), $a = 28.2772(10)$ Å, $b = 11.1135(9)$ Å, $c = 7.9823(3)$ Å, $\beta = 90.234(4)^\circ$, $V = 2508.5(2)$ Å³, $Z = 4$, $T = 100(2)$ K, $\mu(\text{Cu K}\alpha) = 0.728$ mm⁻¹, $D_{\text{calc}} = 1.256$ g/cm³, 19257 reflections measured ($7.956^\circ \leq 2\theta \leq 145.31^\circ$), 4894 unique ($R_{\text{int}} = 0.0918$, $R_{\text{sigma}} = 0.0957$) which were used in all calculations. The final R_1 was 0.0661 ($I > 2\sigma(I)$) and wR_2 was 0.2088 (all data).

Figure S9: Packing diagram viewed down the b axis showing intermolecular hydrogen-bonding interactions (green dots). All hydrogens in the packing diagram have been omitted for clarity, except those involved in hydrogen bonding interactions.

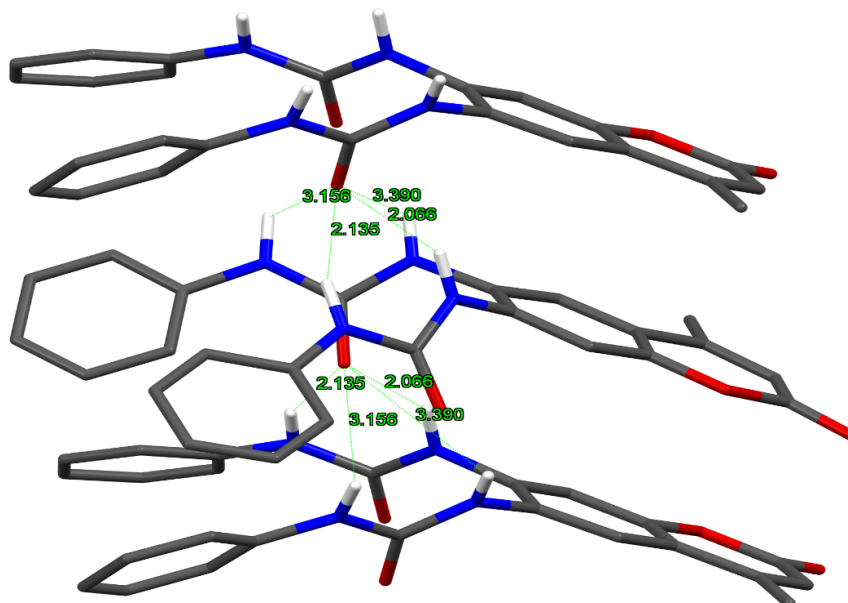
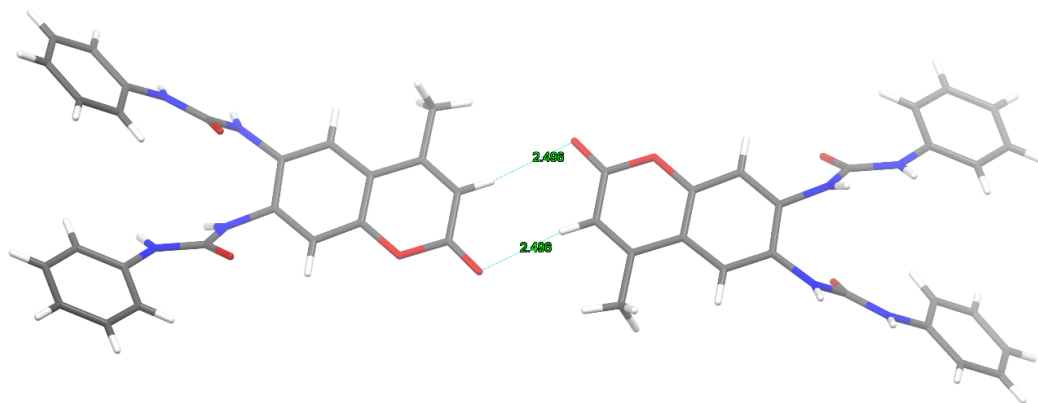


Figure S10: Packing diagram showing intermolecular electrostatic attraction (cyan dots) or receptor 1.



S5. ¹H NMR Titration Binding Studies with TBACl

Proton NMR titration binding studies were performed on Bruker 400 MHz FT-NMR spectrometer at 298 K. Solution of receptors **1-4** in DMSO-*d*₆/0.5% H₂O were prepared in 2 mM concentrations. The guest anion, tetra-*n*-butylammonium (TBA) chloride, was prepared with the same receptor solution, to ensure the overall receptor concentration stays constant whilst the guest anion concentration changes. Using small aliquots of the guest salt, the receptor solution was titrated, and after each addition, chemical shifts were reported in ppm in reference to residual solvent peaks. The isotherm based on the four NH chemical shifts were globally fitted using the online fitting program Bindfit.⁶

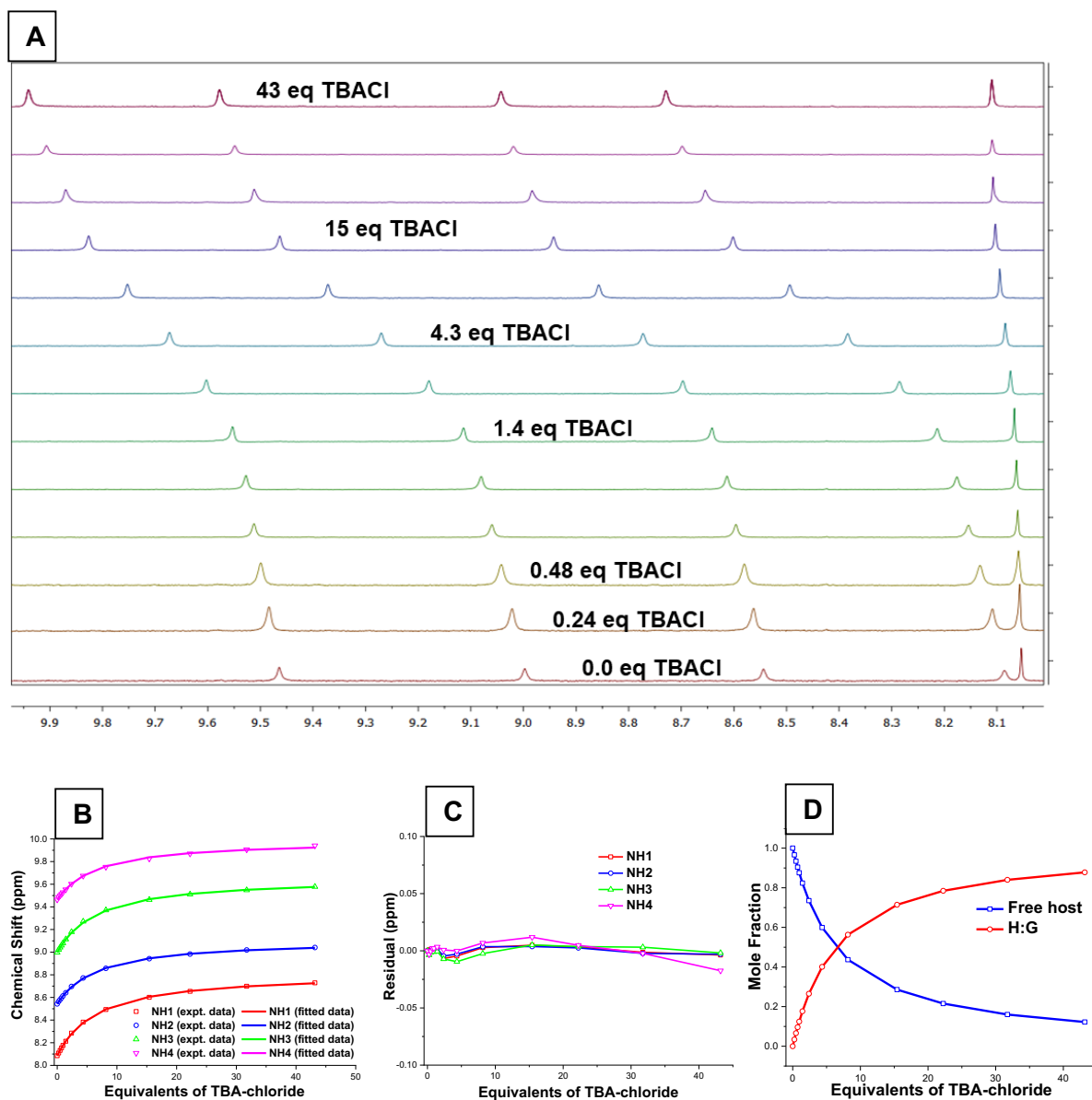


Figure S11: ^1H NMR spectroscopic titration of receptor **1** (2 Mm) with TBACl in $\text{DMSO-}d_6$ with 0.5% water at 298 K. (a) Stack plot. (b) Fitplot for 4 NH protons at $\delta = 8.09, 8.54, 9.00$ and 9.46 ppm using global analysis with 1:1 ($K_a = 81 \text{ M}^{-1}$, error: 1%). (c) Plot of the residuals for using global analysis. (d) Calculated mole fractions.

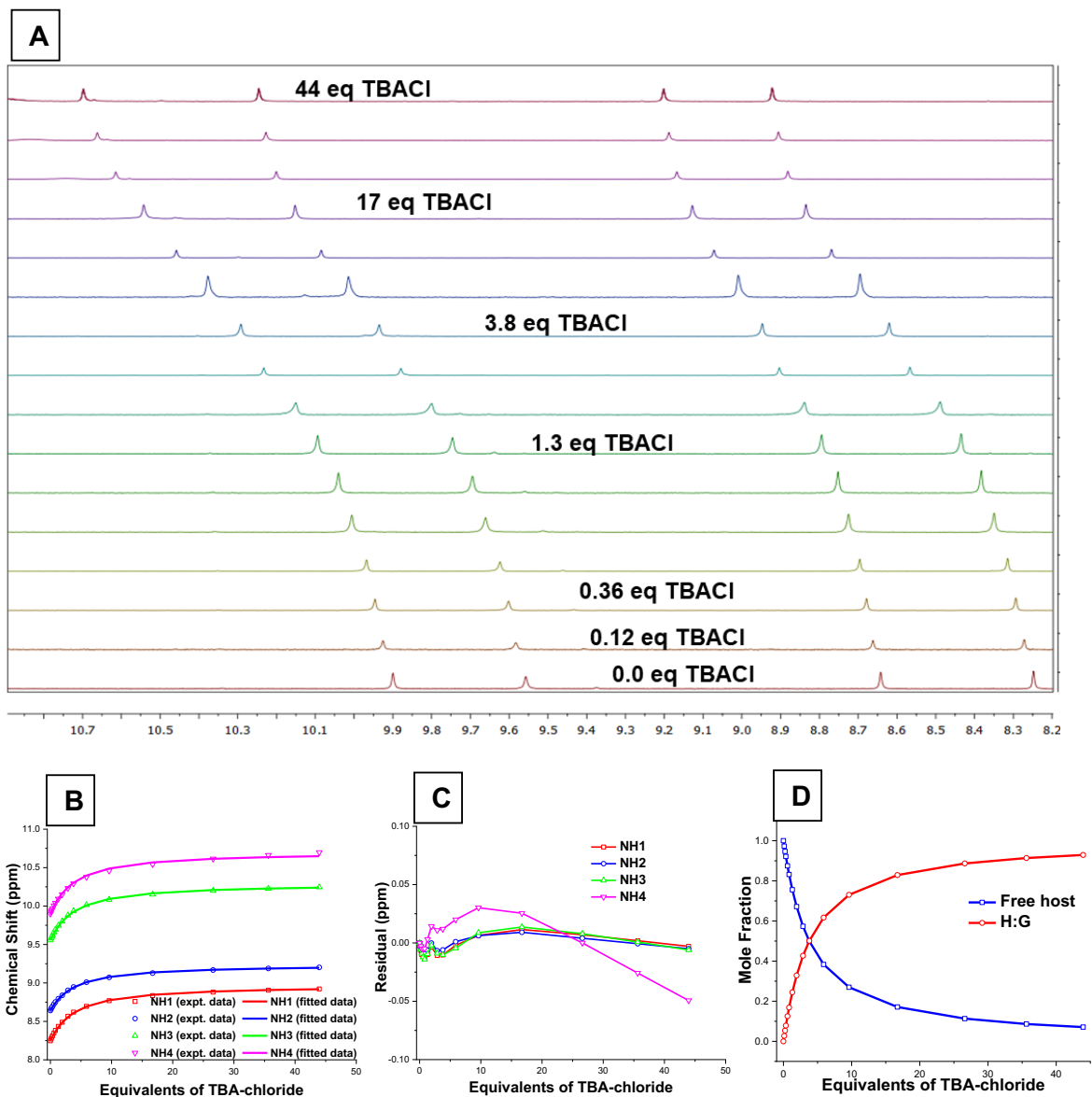


Figure S12: ^1H NMR spectroscopic titration of receptor **2** (2 Mm) with TBACl in $\text{DMSO-}d_6$ with 0.5% water at 298 K. (a) Stack plot. (b) Fitplot for 4 NH protons at $\delta = 8.25, 8.64, 9.56$ and 9.90 ppm using global analysis with 1:1 ($K_a = 146 \text{ M}^{-1}$, error: 3%). (c) Plot of the residuals for using global analysis. (d) Calculated mole fractions.

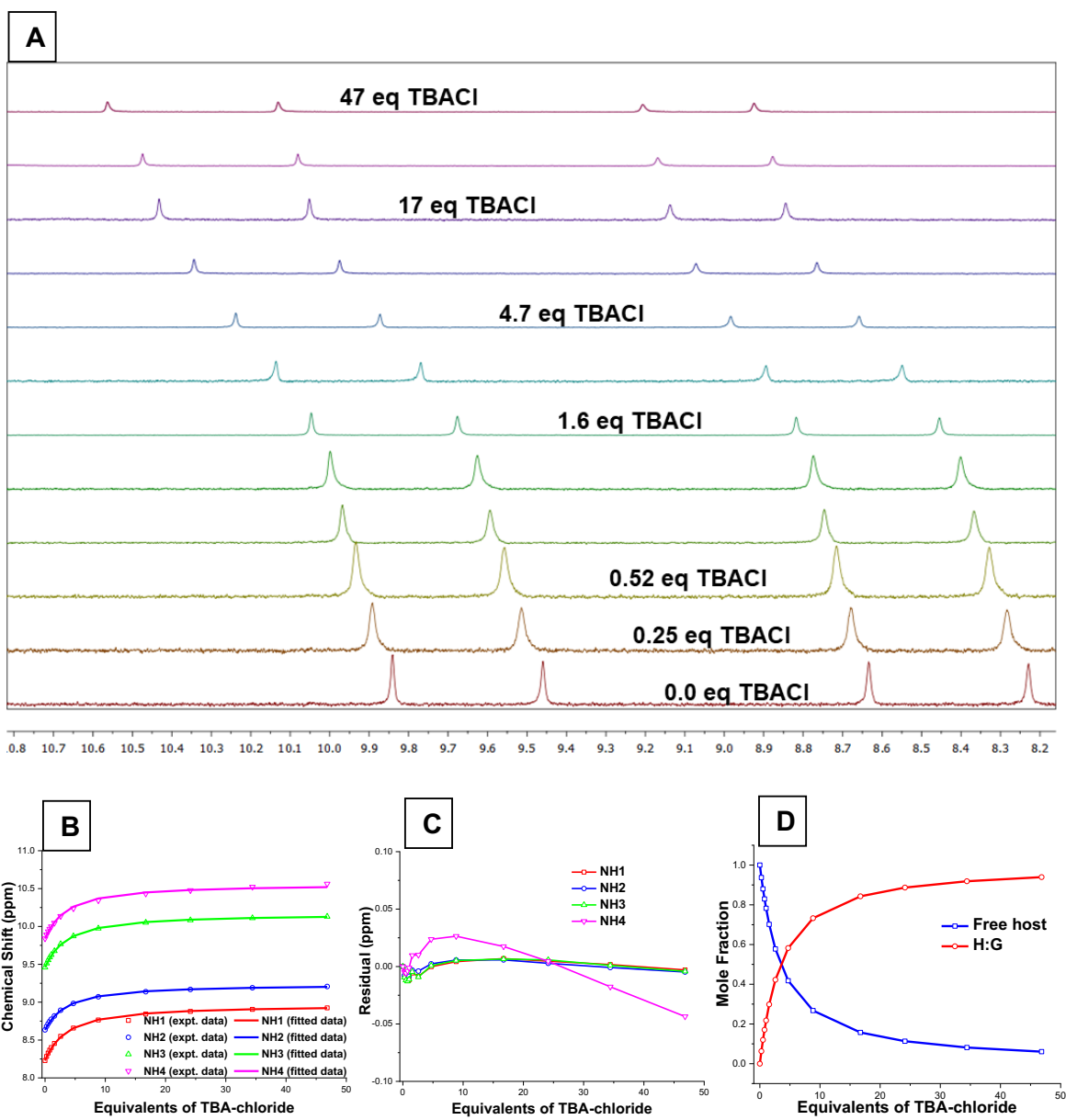


Figure S13: ^1H NMR spectroscopic titration of receptor **3** (2 Mm) with TBACl in $\text{DMSO-}d_6$ with 0.5% water at 298 K. (a) Stack plot. (b) Fitplot for 4 NH protons at $\delta = 8.23, 8.63, 9.46$ and 9.84 ppm using global analysis with 1:1 ($K_a = 177 \text{ M}^{-1}$, error: 3%). (c) Plot of the residuals for using global analysis. (d) Calculated mole fractions.

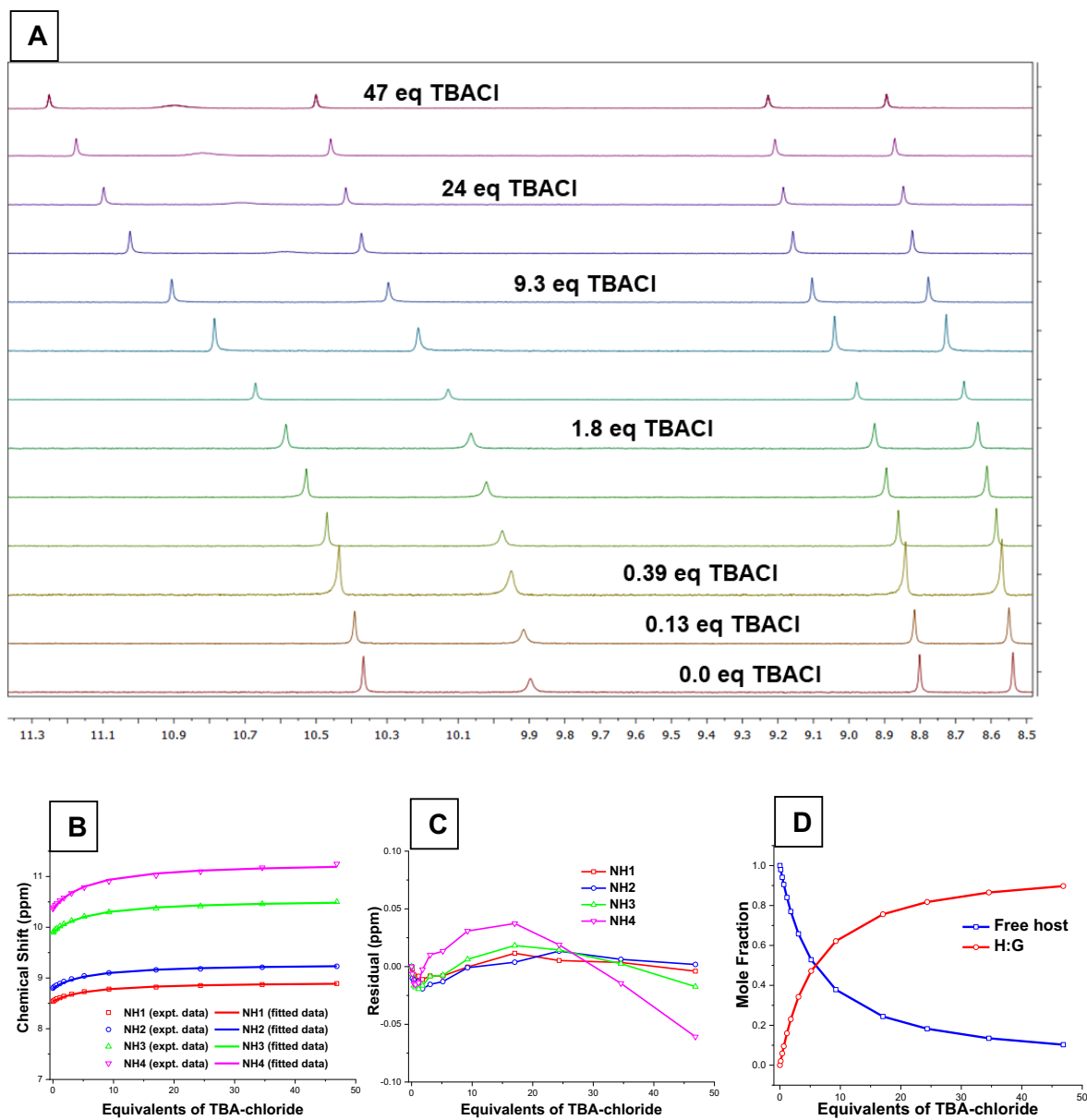


Figure S14: ^1H NMR spectroscopic titration of receptor **4** (2 Mm) with TBACl in $\text{DMSO-}d_6$ with 0.5% water at 298 K. (a) Stack plot. (b) Fitplot for 4 NH protons at $\delta = 8.54, 8.80, 9.90$ and 10.37 ppm using global analysis with 1:1 ($K_a = 96 \text{ M}^{-1}$, error: 5%). (c) Plot of the residuals for using global analysis. (d) Calculated mole fractions.

S6. Anion Transport Studies

S6.1: Ion selective electrode (ISE) assays:

a- Cl/NO₃ exchange assay:

Unilamellar vesicles were prepared as reported.⁷⁻⁹ Briefly, ~ 30 mg of POPC (1-palmitoyl-2-oleoylphosphatidylcholine) was dissolved in 1 mL chloroform in a round-bottomed flask and the solvent was removed in *vacuo* to form a thin lipid layer. The thin film was dried under high vacuum for at least 6 h and was suspended on the internal solution (4 mL) and vortexed using a lab dancer to form large multilamellar vesicles, which was subjected to nine freeze-thaw cycles alternating between water (at room temperature) and liquid nitrogen. Further, the formed lipid was left to rest for 30 minutes and then subjected to extrusion through a 200 nm polycarbonate membranes 25 times to form the unilamellar vesicles. The formed vesicles were subjected to dialysis for 4 h in the desired external solution to remove any unencapsulated internal salts. Finally, using the required external solution, the lipid was diluted to 1.0 mM. The pH of the internal and external solutions was maintained at 7.2 using phosphate buffer with a 500 mM total ionic strength. Test compound in DMSO (10 µL) was added to start the experiment and chloride selective electrode was used to monitor the chloride efflux. Detergent (50 µL) was added after 300 seconds to lyse the vesicles, while the 100% chloride efflux reading was taken at 420 seconds.

- Hill plots for Cl/NO₃:

Hill plots were performed for Cl/NO₃ exchange assay by conducting transport assay at different concentrations of tested compounds. Receptor concentration vs chloride efflux at 270 s (the endpoint of transport assay) were plotted and fitted to the Hill equation using Origin 2019b:

$$y = V_{max} \frac{x^n}{k^n + x^n} = 100\% \frac{x^n}{(EC_{50})^n + x^n}$$

Where y is the chloride efflux at 270 s (%) and x is the tested compound concentration (mol% relative to lipid concentration)

V_{\max} is the maximum efflux possible and considered as 100% as this is experimentally the maximum chloride efflux possible.

k (EC_{50} value) is the carrier concentration needed to reach $V_{\max}/2$.

Each data point on each Hill plot are an average of at least two repeated runs. Error bars represent standard deviation about the mean.

b- KCl efflux – cationohore coupling:

In this assay, 300 mM total ionic strength of both K gluconate external solution and KCl internal solution were maintained. The vesicles were made in a similar way to Cl/NO₃ exchange assay except that gel filtration, using sephadex, replaced dialysis to allow exchange of any unencapsulated KCl for KGlu. External KGlu solution (10 mL) was used to dilute the lipid solution obtained after sephadex to obtain a lipid stock of known concentration. A cationohore, monensin or valinomycin, (10 μ L, 0.5 mM) was added first to the lipid solution at concentration 0.1 mol% with respect to lipid concentration. Then, receptor was added after 30 seconds of the cationohore addition to start the experiment.

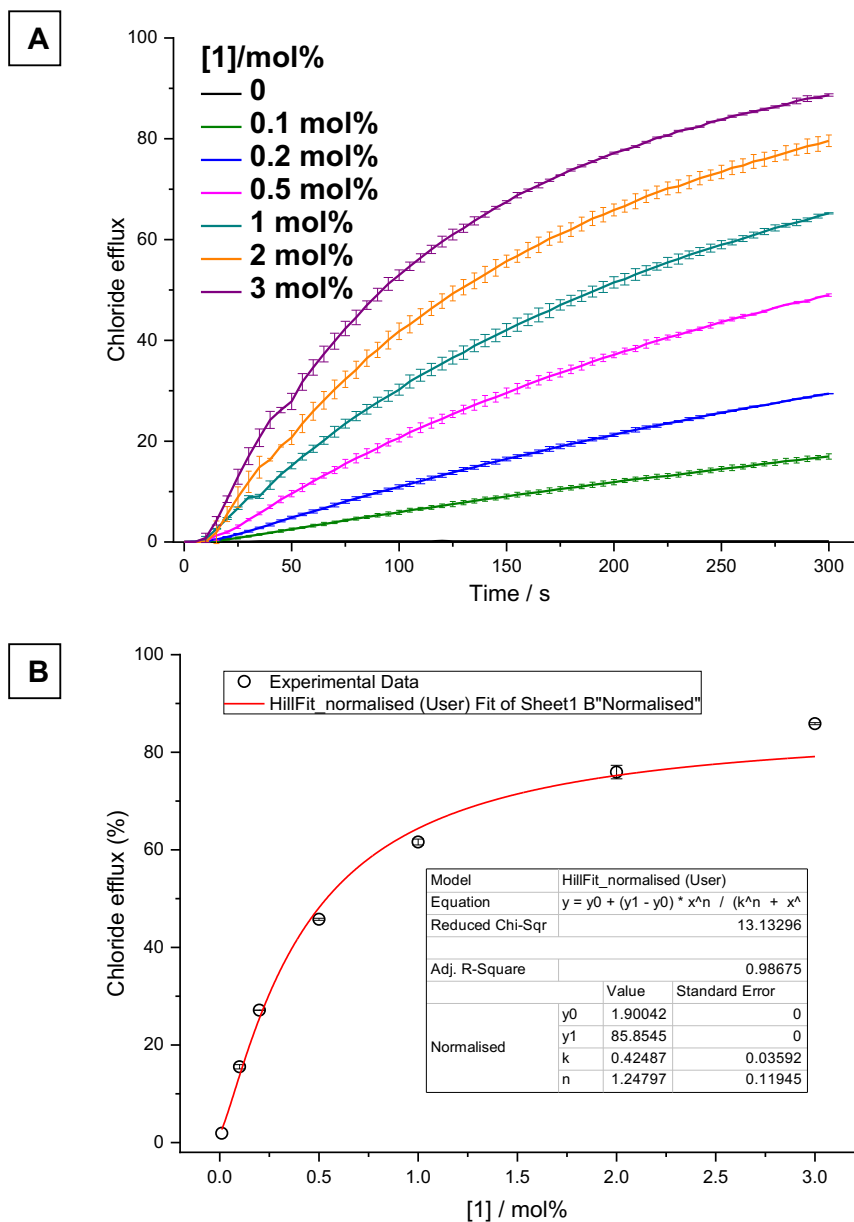


Figure S15: A-Dose response curve and B- Hill plot analysis of chloride efflux facilitated by compound **1** from unilamellar POPC vesicles that were loaded with a 489 mM KCl solution buffered to pH 7.2 with 5 mM phosphate, and were suspended in a 489 mM KNO₃ solution buffered to pH 7.2 with 5 mM phosphate salts. DMSO was used as a control. Each point is the average of at least two repeats.

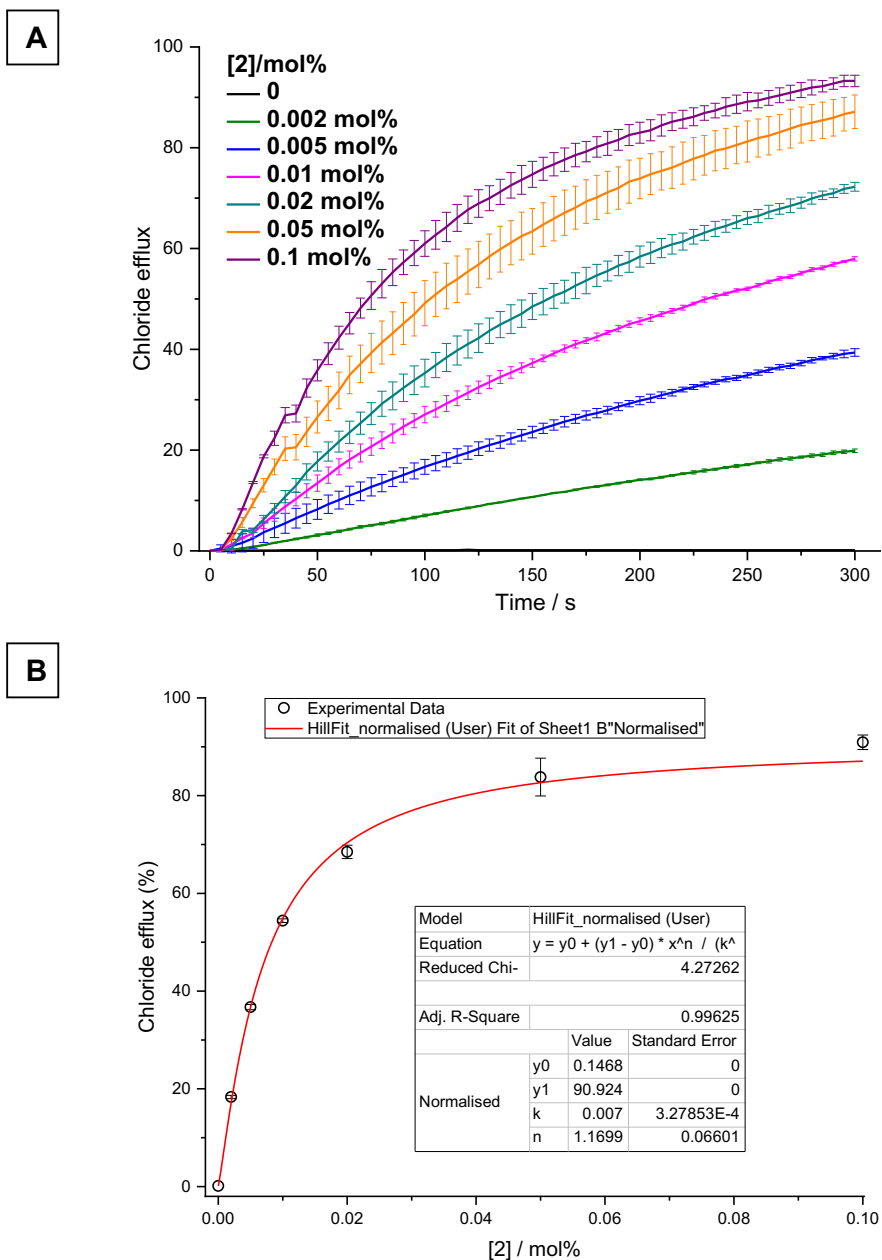


Figure S16: A-Dose response curve and B- Hill plot analysis of chloride efflux facilitated by compound **2** from unilamellar POPC vesicles that were loaded with a 489 mM KCl solution buffered to pH 7.2 with 5 mM phosphate, and were suspended in a 489 mM KNO₃ solution buffered to pH 7.2 with 5 mM phosphate salts. DMSO was used as a control. Each point is the average of at least two repeats.

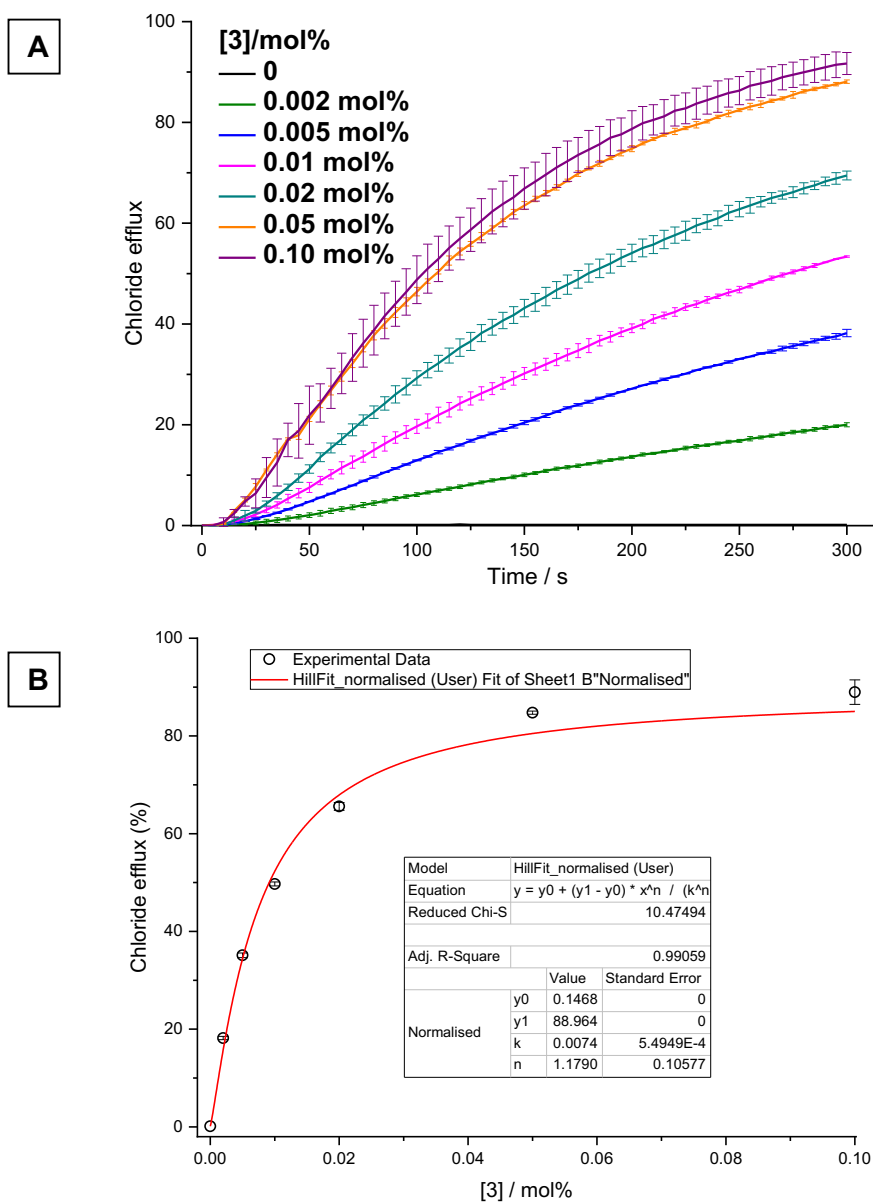


Figure S17: A-Dose response curve and B- Hill plot analysis of chloride efflux facilitated by compound **3** from unilamellar POPC vesicles that were loaded with a 489 mM KCl solution buffered to pH 7.2 with 5 mM phosphate, and were suspended in a 489 mM KNO₃ solution buffered to pH 7.2 with 5 mM phosphate salts. DMSO was used as a control. Each point is the average of at least two repeats.

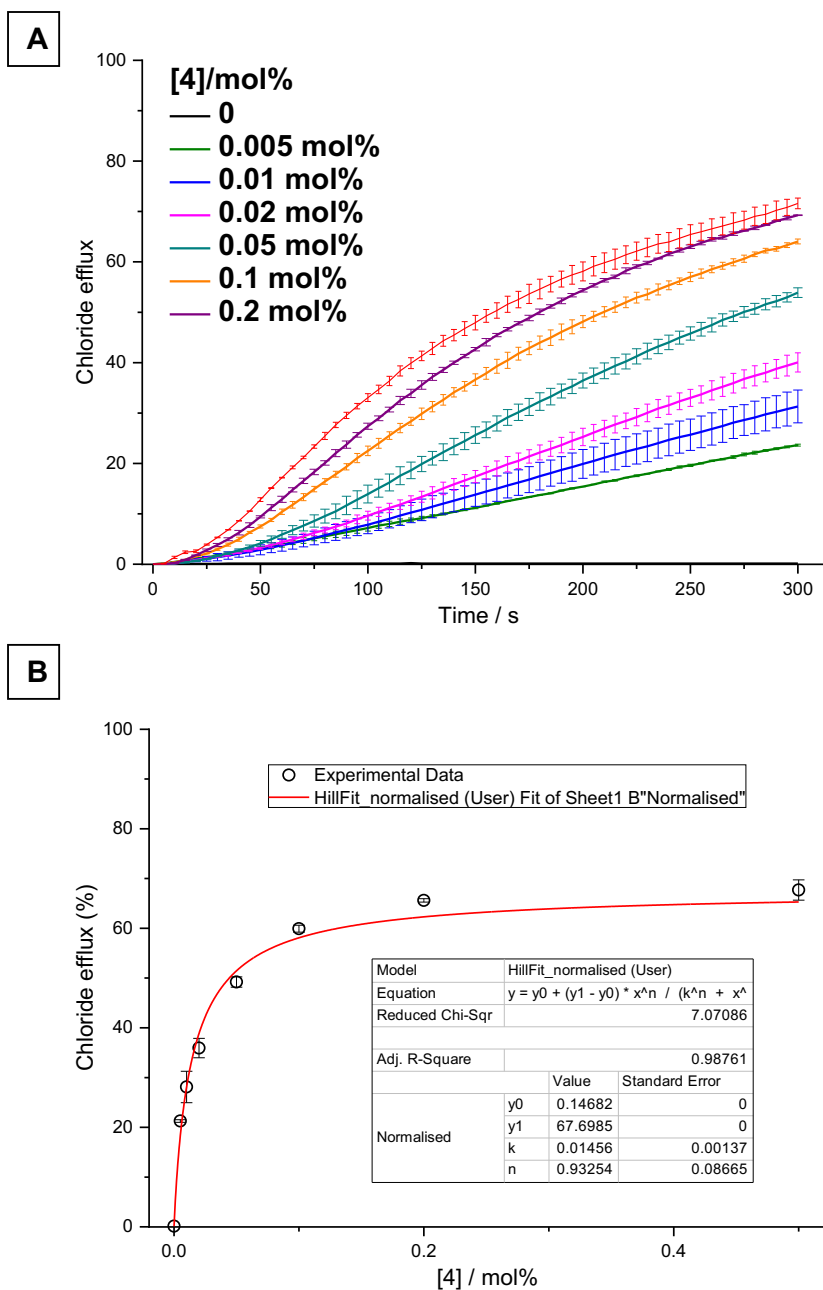


Figure S18: A-Dose response curve and B- Hill plot analysis of chloride efflux facilitated by compound **4** from unilamellar POPC vesicles that were loaded with a 489 mM KCl solution buffered to pH 7.2 with 5 mM phosphate, and were suspended in a 489 mM KNO₃ solution buffered to pH 7.2 with 5 mM phosphate salts. DMSO was used as a control. Each point is the average of at least two repeats.

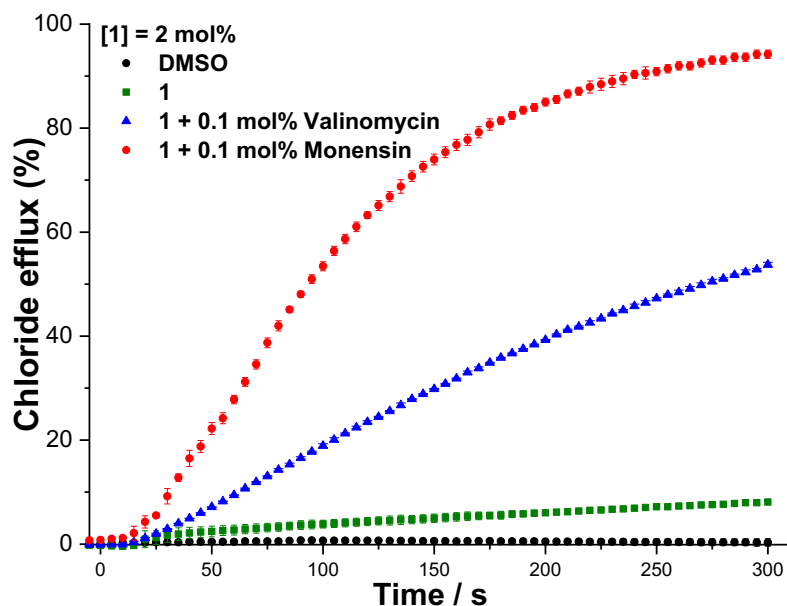


Figure S19: Electrogenic or electroneutral transport mediated by compound **1** (2 mol% with respect to lipid) in the presence of monensin or valinomycin (0.1 mol% with respect to lipid). Unilamellar POPC vesicles were loaded with a 300 mM KCl solution buffered to pH 7.2 with 5 mM phosphate and were suspended in a 300 mM KGluc solution buffered to pH 7.2 with 5 mM phosphate salts. DMSO was used as a control. Each point is the average of at least two repeats.

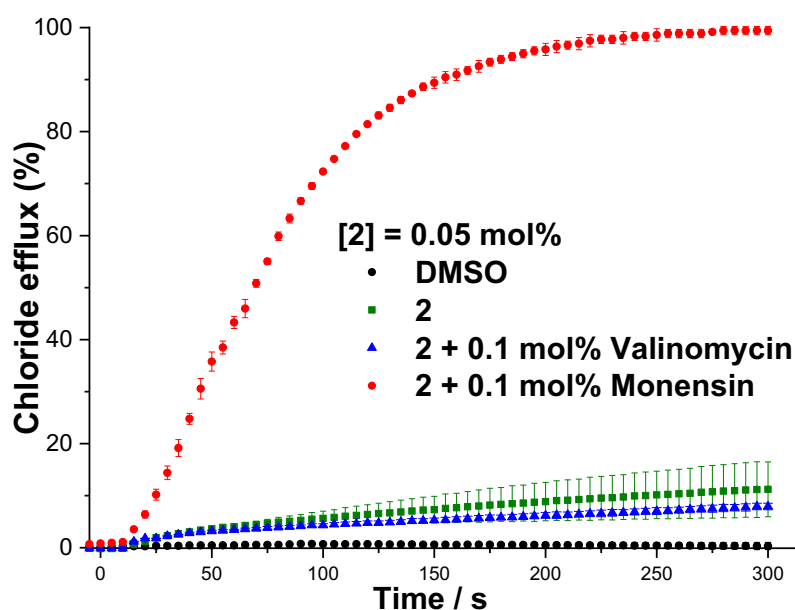


Figure S20: Electrogenic or electroneutral transport mediated by compound **2** (0.05 mol% with respect to lipid) in the presence of monensin or valinomycin (0.1 mol% with respect to lipid). Unilamellar POPC vesicles were loaded with a 300 mM KCl solution buffered to pH 7.2 with 5 mM phosphate and were suspended in a 300 mM KGluc solution buffered to pH 7.2 with 5 mM phosphate salts. DMSO was used as a control. Each point is the average of at least two repeats.

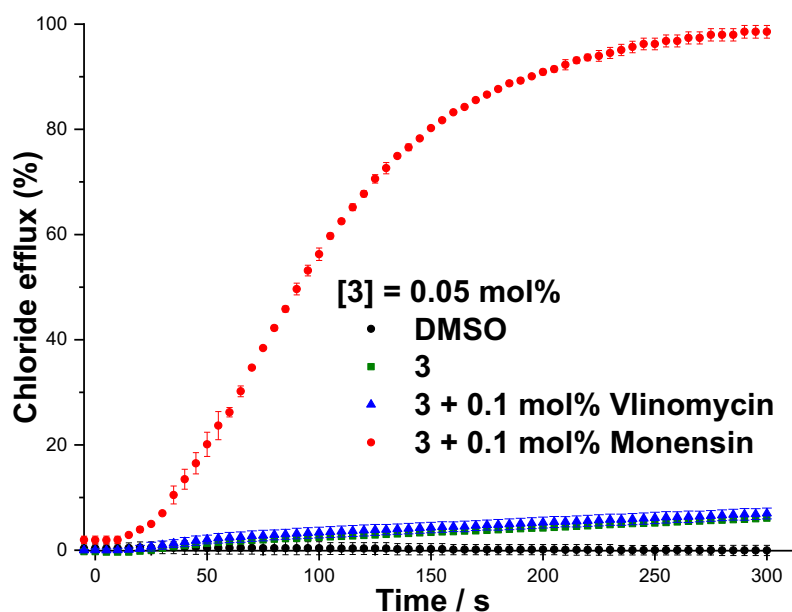


Figure S21: Electrogenic or electroneutral transport mediated by compound **3** (0.05 mol% with respect to lipid) in the presence of monensin or valinomycin (0.1 mol% with respect to lipid). Unilamellar POPC vesicles were loaded with a 300 mM KCl solution buffered to pH 7.2 with 5 mM phosphate and were suspended in a 300 mM K₂Glu solution buffered to pH 7.2 with 5 mM phosphate salts. DMSO was used as a control. Each point is the average of at least two repeats.

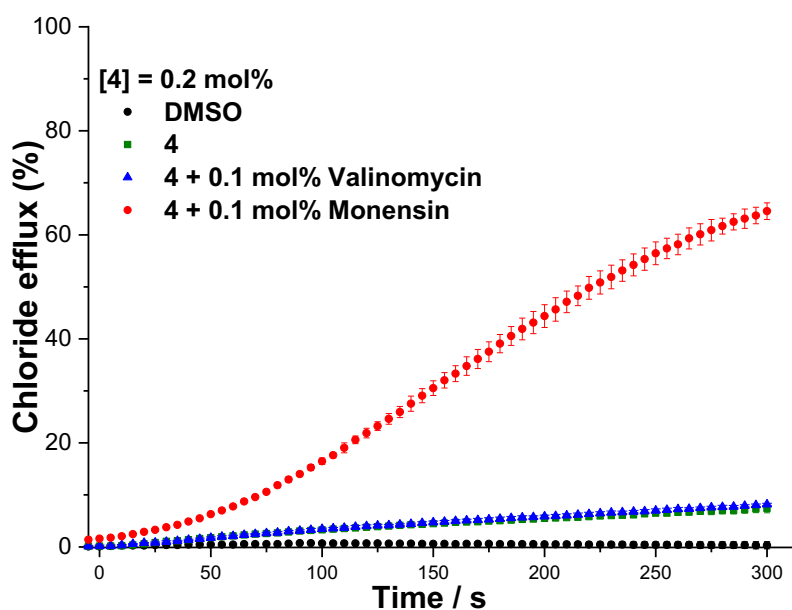


Figure S22: Electrogenic or electroneutral transport mediated by compound **4** (0.2 mol% with respect to lipid) in the presence of monensin or valinomycin (0.1 mol% with respect to lipid). Unilamellar POPC vesicles were loaded with a 300 mM KCl solution buffered to pH 7.2 with 5 mM phosphate and were suspended in a 300 mM K₂Glu solution buffered to pH 7.2 with 5 mM phosphate salts. DMSO was used as a control. Each point is the average of at least two repeats.

S6.2: General preparation for HPTS assays:

Base-pulse 8-hydroxypyrene-1,3,6-trisulfonic acid trisodium salt (HPTS) assays were conducted using unilamellar 1-palmitoyl-2-oleoylphosphatidylcholine vesicles (POPC) with a mean diameter of 200 nm loaded with the pH sensitive fluorescence dye HPTS (1 mM).⁷⁻⁹ A chloroform solution of POPC (~ 30 mg/mL) was evaporated under vacuum and dried for at least 6 h. The thin film was hydrated by the internal solution containing HPTS (1 mM) and was subjected to nine freeze-thaw cycles followed by extrusion 25 times through a 200 nm polycarbonate membrane. Size exclusion chromatography using sephadex G-25 column and HPTS-free external solution as an eluent was conducted to remove untrapped HPTS from the vesicles' solution. The internal and external solutions used were identical salt solution potassium chloride KCl (100 mM) buffered with 10 mM HEPES at pH 7.0. Finally, for each measurement, external solution (KCl) was used to dilute the lipid stock to obtain 2.5 mL lipid suspension containing 0.1 mM lipid. A base pulse of KOH (25 μ L, 0.5 M) at final concentration 5 mM was added to generate a transmembrane pH gradient. After the tested receptors were added, HPTS fluorescence ratio ($\lambda_{\text{ex}} = 460$ nm, $\lambda_{\text{em}} = 510$ nm divided by $\lambda_{\text{ex}} = 403$ nm, $\lambda_{\text{em}} = 510$ nm) was recorded. Assisting ionophore (carbonyl cyanide phenylhydrazone (CCCP) or valinomycin) was used as a 5 μ L DMSO. Bovine serum albumins (BSA) was added to vesicles at 1 mol% (with respect to lipid) and allowed to stir for 30 minutes to test if the transport is fatty acid independent, while, oleic acid (1 mol%) was used as a source of fatty acid to test if the transport is fatty acid dependent. Detergent (25 μ L) was added at 200 seconds to destroy the pH gradient to calibrate the assay.

Results are the average of at least three repeats and the fractional fluorescence intensity (I_f) was determined using the following formula:

$$I_f = \frac{R_t - R_0}{R_d - R_0}$$

Where

- R_t is the fluorescence ratio at time t.

- R_0 is the fluorescence ratio at time 0
- R_d is the fluorescence ratio after detergent addition.

Hill plots were determined for KCl transport assay by conducting transport assays at different tested receptors concentrations. Receptor concentration vs fractional fluorescence intensity I_f at 200 s (the endpoint of transport assay) were plotted and fitted to the Hill equation using Origin 2019b:

The following formula was used to calculate hill coefficients (n) and EC_{50} (200 s) values by fitting the curves to the following equation:

$$y = y_0 + (y_{max} - y_0) \frac{x^n}{K^n + x^n}$$

Where:

- y is I_f (200 s) value of the ionophore at concentration x (receptors concentration is expressed as ionophore to lipid molar ratio).
- y_0 is I_f value at 200 s, without addition of the ionophore.
- y_{max} is the maximum I_f value.
- n is the Hill coefficient, and K is the EC_{50} (200 s) value.

HPTS-based assays

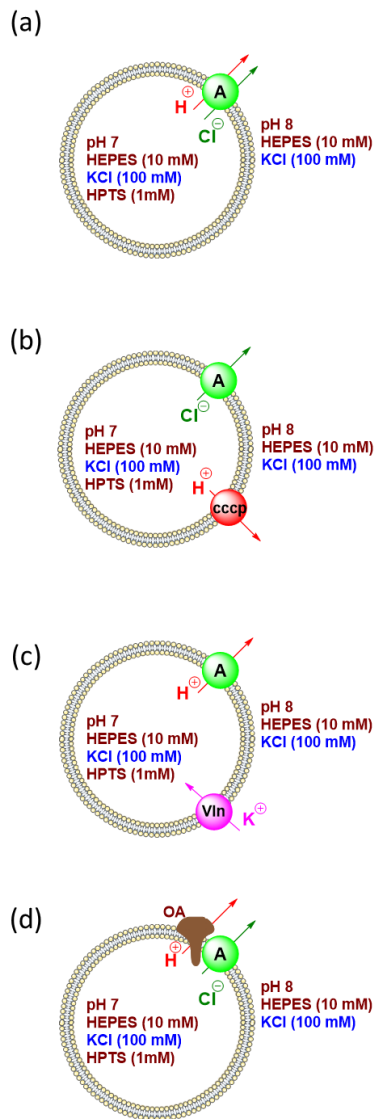


Figure S23: Schematic representation of the HPTS-based assays used in the current study (a) H^+ /Cl⁻ symport or OH⁻/Cl⁻ antiport (b) the presence of cccp (protonophore) to assess Cl⁻ uniport (c) the presence of valinomycin to measure the proton flux (d) the effect of fatty acid presence as a fuel on the transport.

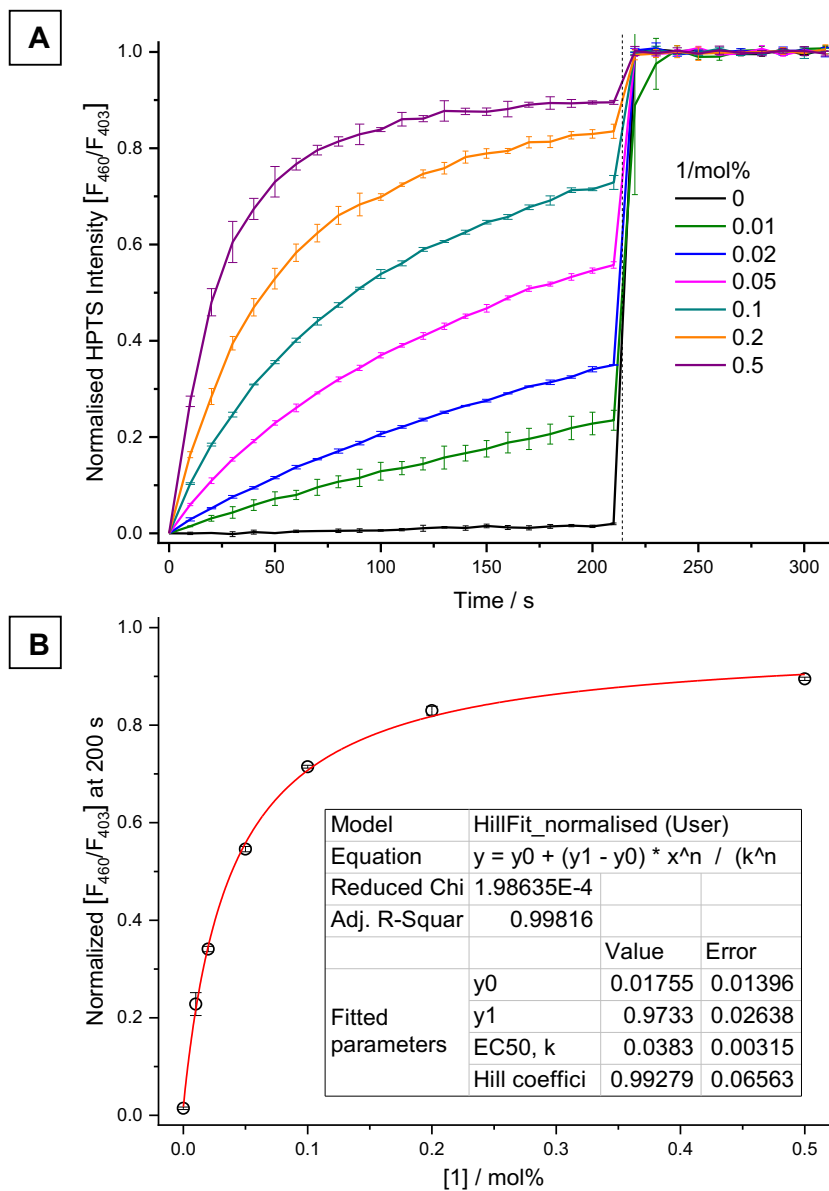


Figure S24: A-Dose response curve, B-Hill plot analysis of H^+/Cl^- symport or Cl^-/OH^- antiport facilitated by compound **1** using KCl-KOH assay from POPC vesicles loaded with KCl (100 mM), buffered to pH 7.0 with HEPES (10 mM). The test compound was added at 0 s and detergent was added at 200 s. Ionophore concentrations are shown as ionophore to lipid molar ratios. Error bars represent SD from at least three repeats.

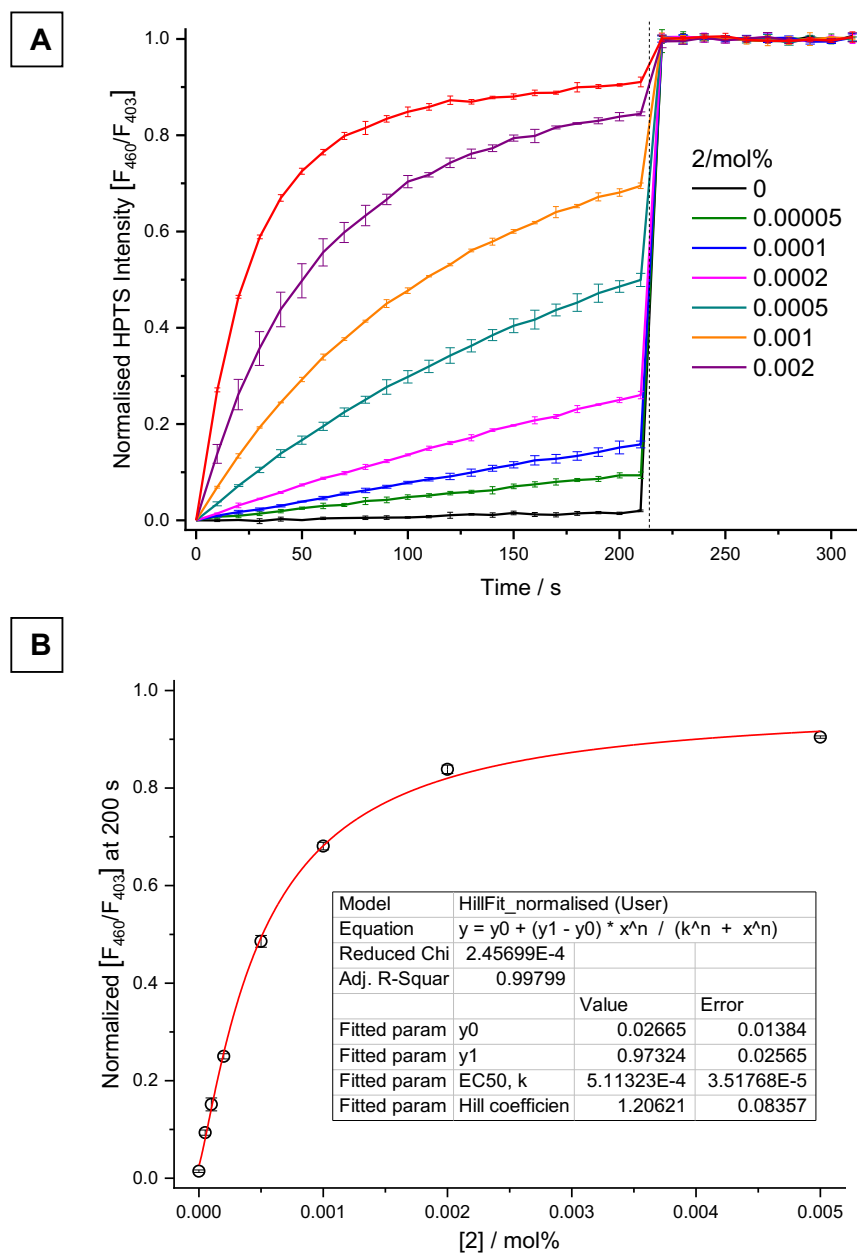


Figure S25: A-Dose response curve, B-Hill plot analysis of H^+/Cl^- symport or Cl^-/OH^- antiport facilitated by compound **2** using KCl-KOH assay from POPC vesicles loaded with KCl (100 mM), buffered to pH 7.0 with HEPES (10 mM). The test compound was added at 0 s and detergent was added at 200 s. Ionophore concentrations are shown as ionophore to lipid molar ratios. Error bars represent SD from at least three repeats.

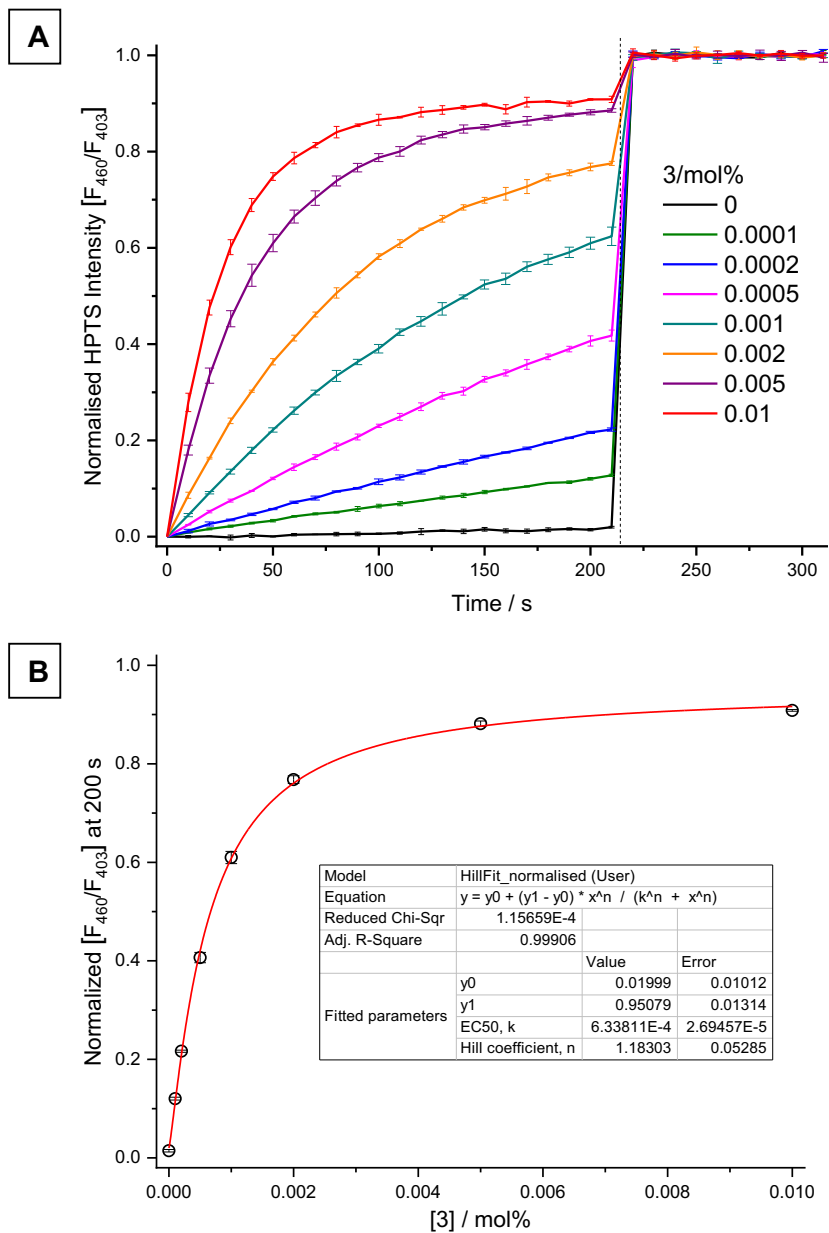


Figure S26: A-Dose response curve, B-Hill plot analysis of H^+/Cl^- symport or Cl^-/OH^- antiport facilitated by compound **3** using KCl-KOH assay from POPC vesicles loaded with KCl (100 mM), buffered to pH 7.0 with HEPES (10 mM). The test compound was added at 0 s and detergent was added at 200 s. Ionophore concentrations are shown as ionophore to lipid molar ratios. Error bars represent SD from at least three repeats.

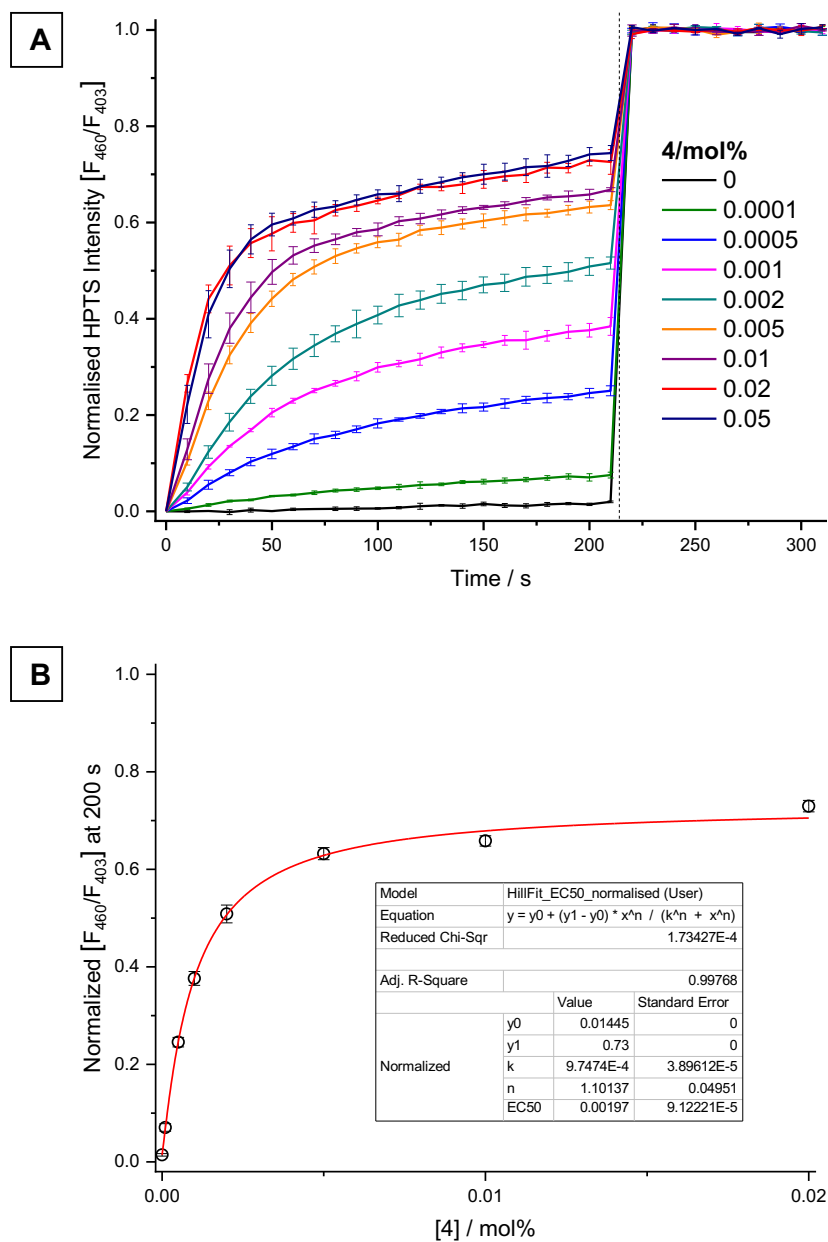


Figure S27: A-Dose response curve, B-Hill plot analysis of H^+/Cl^- symport or Cl^-/OH^- antiport facilitated by compound **4** using KCl-KOH assay from POPC vesicles loaded with KCl (100 mM), buffered to pH 7.0 with HEPES (10 mM). The test compound was added at 0 s and detergent was added at 200 s. Ionophore concentrations are shown as ionophore to lipid molar ratios. Error bars represent SD from at least three repeats.

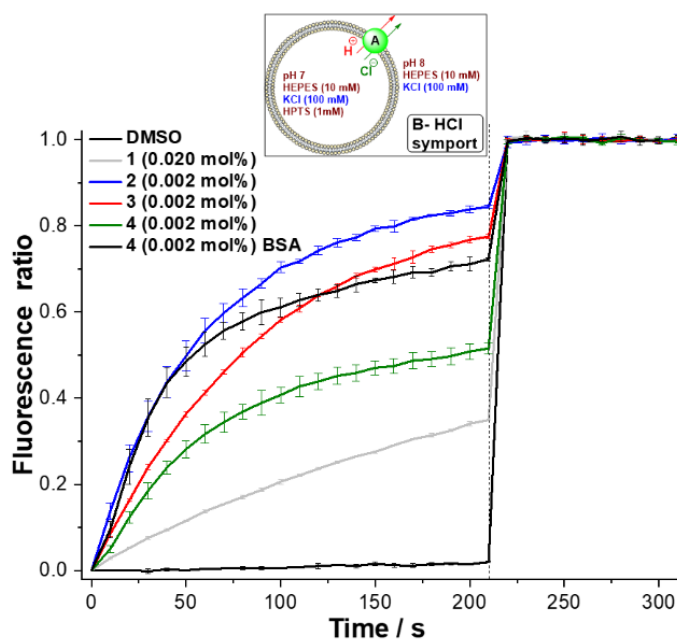


Figure S28; H^+/Cl^- symport or OH^-/Cl^- antiport facilitated by compounds **1–4** (0.02 mol% (rtl) for transporter **1** and 0.002 mol% (rtl) for transporters **2–4**) from unilamellar POPC vesicles loaded with 100 mM KCl buffered to pH 7.0 with 10 mM HEPES buffer and 1 mM HPTS internal sensor. and suspended in an external solution of 100 mM KCl buffered to pH 7.0 with 10 mM HEPES buffer. At 200 s, the detergent was added to lyse the vesicles and collapse the pH gradient for calibration of HPTS fluorescence. Transporter **4** was tested in the presence of BSA-treated lipids. DMSO was used as a control experiment.

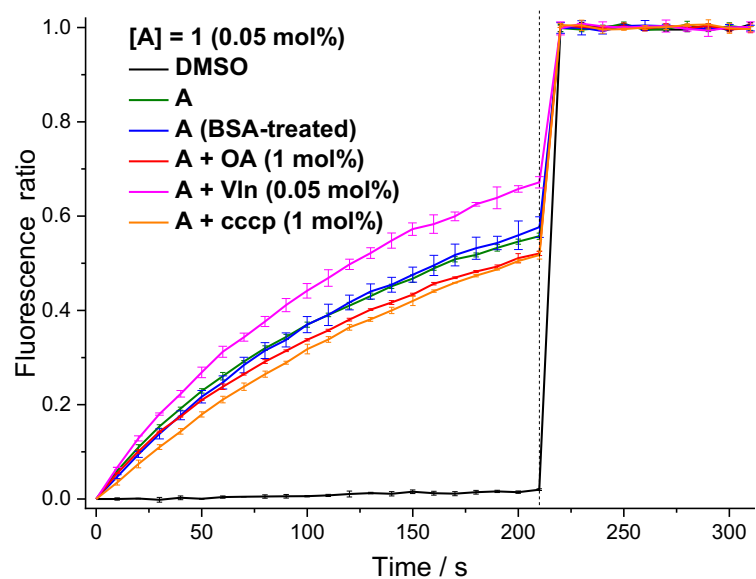


Figure S29: Using KCl-KOH assay from POPC vesicles loaded with KCl (100 mM), buffered to pH 7.0 with HEPES (10 mM), different conditions were applied including using BSA-treated lipid (to test if the transport is fatty acid dependent) addition of oleic acid at 1 mol% (as a source of fatty acid), addition of the protonophore cccp at 1 mol% (to measure of chloride uniport solely), or addition of valinomycin at 0.05 mol% (as a measure of H^+ flux), on the rate of chloride transport of receptor **1** (0.05 mol%).

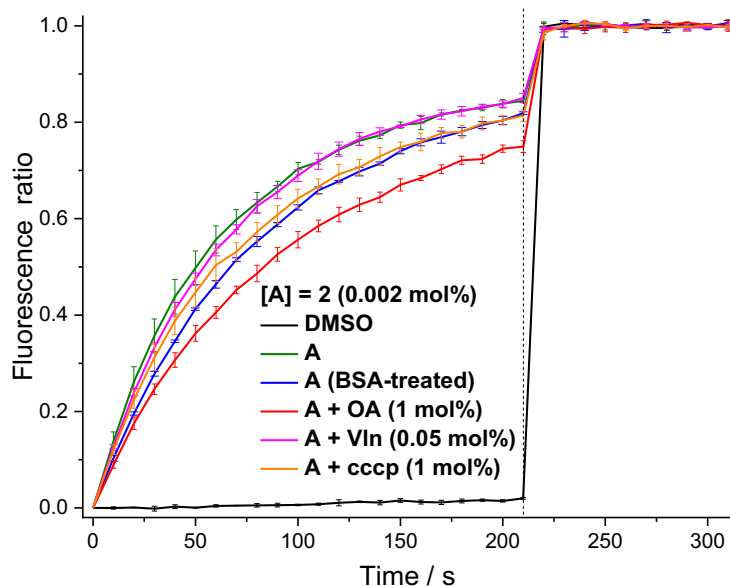


Figure S30: Using KCl-KOH assay from POPC vesicles loaded with KCl (100 mM), buffered to pH 7.0 with HEPES (10 mM), different conditions were applied including using BSA-treated lipid (to test if the transport is fatty acid dependent) addition of oleic acid at 1 mol% (as a source of fatty acid), addition of the protonophore cccp at 1 mol% (to measure of chloride uniport solely), or addition of valinomycin at 0.05 mol% (as a measure of H^+ flux), on the rate of chloride transport of receptor **2** (0.002 mol%).

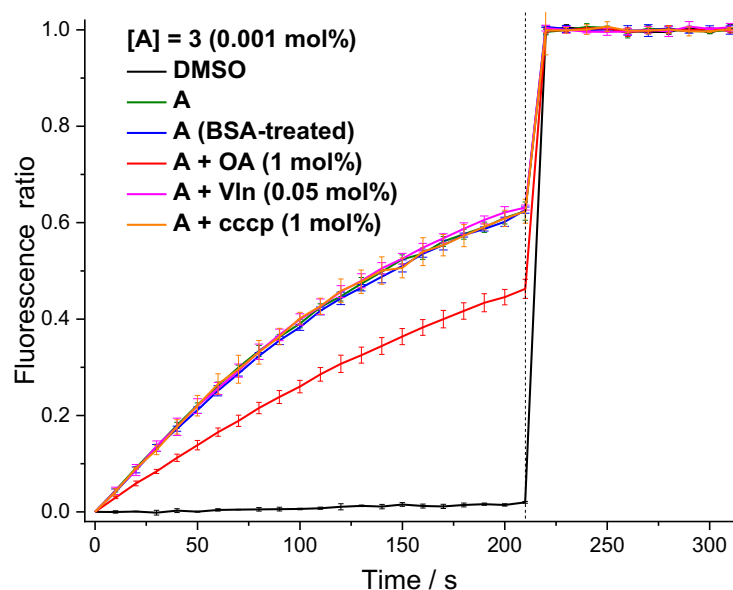


Figure S31: Using KCl-KOH assay from POPC vesicles loaded with KCl (100 mM), buffered to pH 7.0 with HEPES (10 mM), different conditions were applied including using BSA-treated lipid (to test if the transport is fatty acid dependent) addition of oleic acid at 1 mol% (as a source of fatty acid), addition of the protonophore cccp at 1 mol% (to measure of chloride uniport solely), or addition of valinomycin at 0.05 mol% (as a measure of H⁺ flux), on the rate of chloride transport of receptor **3** (0.001 mol%).

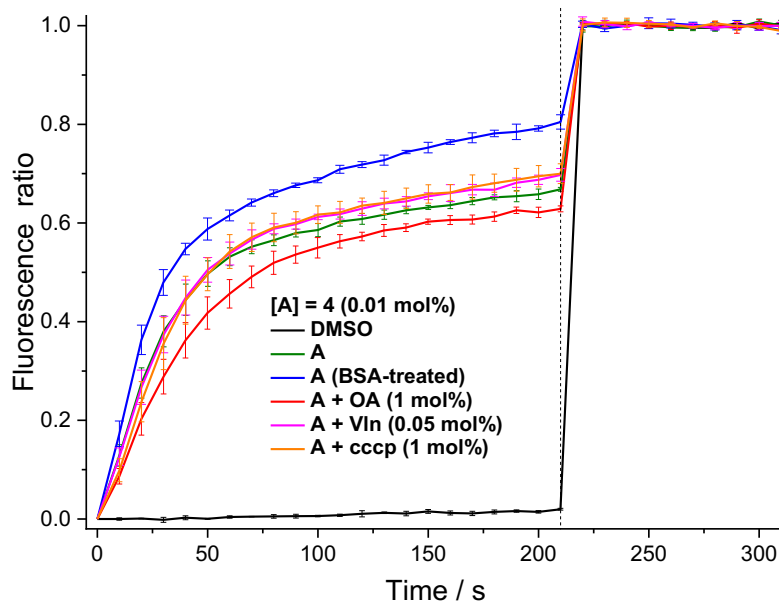


Figure S32: Using KCl-KOH assay from POPC vesicles loaded with KCl (100 mM), buffered to pH 7.0 with HEPES (10 mM), different conditions were applied including using BSA-treated lipid (to test if the transport is fatty acid dependent) addition of oleic acid at 1 mol% (as a source of fatty acid), addition of the protonophore cccp at 1 mol% (to measure of chloride uniport solely), or addition of valinomycin at 0.05 mol% (as a measure of H⁺ flux), on the rate of chloride transport of receptor **4** (0.01 mol%).

S7. Biological results:

General cell culture information:

Human cell lines A549 (lung carcinoma), human colon adenocarcinoma cells (SW620) and MCF-7 (breast adenocarcinoma) were obtained from the American Type Culture Collection (ATCC, Manassas VA) and maintained in DMEM media (Biological Industries, Beit Haemek, Israel) supplemented with 100 U/mL penicillin, 100 µg/mL streptomycin, and 2 mM L-glutamine, all from Biological Industries and 10% fetal bovine serum (FBS; Invitrogen- Life Technologies, Carlsbad, CA). Cells were grown at 37 °C under a 5% CO₂ atmosphere.

7.1 Cell viability assay (MTT)

Cell viability was determined by the MTT assay. Cells (1×10^5 cells/mL) were seeded in 96-well microtiter plates and incubated for 24 h to allow cells to attach. Afterwards, they were treated for 24 h with different compound concentrations to obtain the dose-response curves (range 0.78 to 100 µM) and inhibitory concentration of 50% of cell population (IC₅₀ values) were calculated. Compound diluent (maximum 1% DMSO) was added to control cells. Then, 10 µM of 3-(4,5-dimethylthiazol-2-yl)-2,5-diphenyltetrazolium bromide diluted in PBS (MTT, Sigma-Aldrich, St Louis, MO) was added to each well for an additional 2 h. The medium was removed and the MTT formazan precipitate was dissolved in 100 µl of DMSO. Absorbance was read on a Multiskan multiwell plate reader (Thermo Scientific Inc., Waltham, MA) at 570 nm. For each condition, at least three independent experiments were performed in triplicates. Cell viability was expressed as a percentage of control cells, and data are shown as the mean value \pm S.D. Dose-response curves and IC₅₀ values were calculated with GraphPad Prism 8 software.

Table 1: IC₂₅, IC₅₀ and IC₇₅ values of compounds **1–4** on human lung carcinoma (A549), human colon adenocarcinoma (SW620) and human breast adenocarcinoma (MCF-7) cell lines: (ND = non determined)

		A549	SW620	MCF7
1	IC₇₅	ND	ND	ND
	IC₅₀	ND	ND	ND
	IC₂₅	ND	ND	ND
2	IC₇₅	ND	ND	ND
	IC₅₀	ND	ND	ND
	IC₂₅	ND	ND	ND
3	IC₇₅	ND	ND	ND
	IC₅₀	ND	ND	ND
	IC₂₅	ND	ND	ND
4	IC₇₅	6.06 ± 1.44	0.83 ± 0.09	35.71 ± 11.93
	IC₅₀	1.86 ± 0.39	0.51 ± 0.07	17.92 ± 4.25
	IC₂₅	0.61 ± 0.23	0.32 ± 0.08	9.29 ± 2.41

S8. References:

1. R. L. Atkins and D. E. Bliss, *J. Org. Chem.*, 1978, **43**, 1975-1980.
2. T. S. Reddy and A. R. Reddy, *Dyes Pigm.*, 2013, **96**, 525-534.
3. L. J. Bourhis, O. V. Dolomanov, R. J. Gildea, J. A. Howard and H. Puschmann, *Acta Crystallogr. Sect. A: Found. Adv.*, 2015, **71**, 59-75.
4. O. V. Dolomanov, L. J. Bourhis, R. J. Gildea, J. A. Howard and H. Puschmann, *J. Appl. Crystallogr.*, 2009, **42**, 339-341.
5. G. M. Sheldrick, *Acta Crystallogr. Sect. A: Found. Crystallogr.*, 2008, **64**, 112-122.
6. X. Wu, P. Wang, P. Turner, W. Lewis, O. Catal, D. S. Thomas and P. A. Gale, *Chem*, 2019, **5**, 1210-1222.

7. S. N. Berry, V. Soto-Cerrato, E. N. Howe, H. J. Clarke, I. Mistry, A. Tavassoli, Y.-T. Chang, R. Pérez-Tomás and P. A. Gale, *Chem. Sci.*, 2016, **7**, 5069-5077.
8. X. Wu, L. W. Judd, E. N. Howe, A. M. Withecombe, V. Soto-Cerrato, H. Li, N. Busschaert, H. Valkenier, R. Pérez-Tomás and D. N. Sheppard, *Chem*, 2016, **1**, 127-146.
9. L. A. Jowett, E. N. Howe, X. Wu, N. Busschaert and P. A. Gale, *Chem. Eur. J.*, 2018, **24**, 10475-10487.